FUSION OF HUMAN SERUM ALBUMIN TO HUMAN APOLIPOPROTEIN E PEPTIDE AS A NOVEL INHIBITOR OF HEPATITIS C VIRUS ENTRY

by

Brandon A. Deshmukh

BS, University of Missouri-Kansas City, 2010

Submitted to the Graduate Faculty of

Graduate School of Public Health in partial fulfillment

of the requirements for the degree of

Master of Science

University of Pittsburgh

2012

UNIVERSITY OF PITTSBURGH

GRADUATE SCHOOL OF PUBLIC HEALTH

This thesis was presented

by

Brandon A. Deshmukh

It was defended on

June 12, 2012

and approved by

Jared D. Evans, PhD
Assistant Professor
Microbiology and Molecular Genetics
Center for Vaccine Research
University of Pittsburgh

Salvador Z. Tarun, Jr., PhD
Assistant Professor
Department of Infectious Diseases and Microbiology
Graduate School of Public Health
University of Pittsburgh

Thesis Director: Tianyi Wang, PhD
Assistant Professor
Department of Infectious Diseases and Microbiology
Graduate School of Public Health
University of Pittsburgh

Tianyi Wang, PhD

FUSION OF HUMAN SERUM ALBUMIN TO HUMAN APOLIPOPROTEIN E PEPTIDE AS A NOVEL INHIBITOR OF HEPATITIS C VIRUS ENTRY

Brandon A. Deshmukh, M.S.

University of Pittsburgh, 2012

The hepatitis C virus (HCV) affects an estimated 3% of the world's population making it a major threat to human health. Currently, the most common treatment for those infected with the virus includes a combination of pegylated interferon (IFN-α) with ribavirin. This treatment is effective only 40-80% of the time and causes severe side effects leading to low patient compliance. In 2011, two anti-HCV drugs, telaprevir and boceprevir, were put on the market. Both of these drugs are viral protease inhibitors, and are expected to face drug resistance in the future due to the development of viral quasispecies. Due to the uncertainty and problems the current HCV treatments face, there is an urgent need to develop more effective anti-HCV therapies. The blocking of HCV entry into human hepatocytes has promise. Our lab has already developed a novel anti-HCV peptide called human apolipoprotein E peptide (hEP) which was shown to potently block HCV entry into Huh7.5.1 cells at very low concentrations, as well as lower plasma cholesterol levels and suppress inflammation in mice. At the same time, this peptide was non-toxic to cells. The combination of potently blocking viral entry, as well as maintaining the integrity of the cells treated makes hEP a promising anti-HCV therapeutic. In order to increase the stability of hEP, we believed that fusing it to human serum albumin would increase its pharmacokinetics, shelf life, as well as lower the necessary dosage needed to elicit anti-viral effects. This rationale was based on the findings of another group which showed that the fusion of IFN-α to human serum albumin increased its half-life. The methylotropic yeast

strain X-33 *Pichia pastoris* was used to produce the hEP and human serum albumin recombinant fusion protein. After successfully producing the recombinant proteins of interest, we saw viral inhibition among one of our hEP fusion proteins, demonstrating its efficacy and public health significance.

TABLE OF CONTENTS

LIST OF TABLES

LIST OF FIGURES

ACKNOWLEDGEMENT

I would like to start by thanking my PI Dr. Tianyi Wang for giving me the opportunity to join his lab and gain the research experience I have accumulated during the duration of the program. He has been an exceptional mentor, and I will always be grateful for his knowledge and support. It has been an honor working in his lab. In addition, I would like to thank my committee members Dr. Jared Evans and Dr. Salvador Tarun Jr. for serving on my committee as well as for all the helpful suggestions they have given me. They always agreed to meet with me whenever I needed to. I would also like to thank Dr. Anil Ojha and Kathy Kulka for letting me use their electroporator. This was instrumental in getting the kinds of results I wanted.

The others who made my experience in IDM so valuable are my fellow lab mates Shufeng Liu, Jana Jacobs, Kevin McCormick, Derek Rinchuse, Steven Aussenberg, Aram Lee, and Ting Zhao. They were always there to help me whenever I asked, and teach me whenever I needed to learn new lab techniques. I will always be grateful for their instruction and support. I personally would like to thank Ting for taking the time to perform mass spectrometry on the samples I gave her. The results I got back were very rewarding.

Lastly, I would like to say thank you to my Mom and Dad who have given me nothing less than the utmost support during graduate school. Without their love, support, and encouragement, I would never have made this far in life. They are the two best role models I have.

1.0 INTRODUCTION

1.1 DESCRIPTION OF THE PROBLEM

In 2011, the World Health Organization estimated that 170 million people worldwide were infected with the hepatitis C virus (HCV). HCV leads to cirrhosis of the liver, hepatocellular carcinoma, and potentially liver failure if the person does not seek treatment (47, 85). It is primarily spread through the sharing of needles, but can also be spread via blood transfusion as well as through sexual intercourse. There is currently no prophylactic vaccine for HCV and the current treatment of pegylated interferon (IFN-α) and ribavirin if effective only 40-80% of the time, and causes severe side effects leading to low patient compliance (33). The release of the protease inhibitors boceprevir and telaprevir in 2011 looked to be promising therapeutics for infected individuals, but it is believed that the rise of future viral quasispecies will lead to viral resistance to these drugs (92). This is why new novel anti-viral therapeutics are urgently needed.

1.2 HEPATITIS C VIRUS

HCV is an enveloped positive ssRNA virus which belongs to the family *Flaviviridae* and genus *Hepacivirus*. There are seven viral genotypes, and more than 90 subtypes which are

present in different geographical locations (75). The virus's genetic material is surrounded by an icosahedral shell of the structural protein core (C), and a lipid membrane derived from a host cell as well as two viral-encoded glycoproteins, E1 and E2. The average diameter of an HCV viral particle is around 60 nm and the genome of the virus is 9.6 kilobases with non-translated regions (NTR) within the 5' and 3' ends (Fig. 2). The 5' NCR contains an internal ribosome entry site (IRES) which allows translation of a viral polypeptide in a cap independent fashion (24, 96, 100). When HCV comes into contact with a susceptible cell, it will enter via clathrin-mediated endocytosis into an early endosome (18, 25, 65). This endosome consists of the virus particle

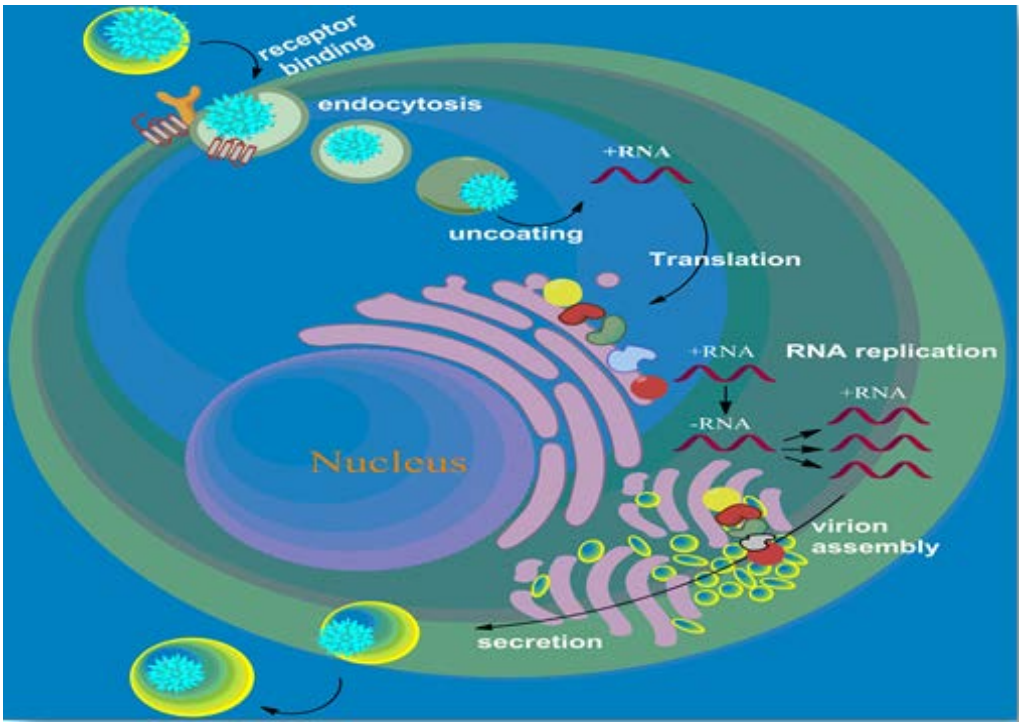

Figure 1. Hepatitis C virus lifecycle Designed by Jana Jacobs

surrounded by the host cell membrane. As the endosome moves further into the cell, it will develop into a late endosome where it is believed that a lowering in pH causes fusion between the viral membrane and surrounding cellular membrane releasing the viral RNA (65, 95). This

assumption is based on findings from another *Flavivirus*, dengue, and the *Alphavirus*, Semliki Forest virus, in which low pH causes membrane fusion (39, 68). Since the HCV RNA genome is positive stranded, it can be translated right away. Once it is translated, the individual proteins associate into the endoplasmic reticulum membrane and form replication vesicles (41). It is within these replication vesicles where genome replication takes place as well as particle assembly. Once particle assembly is complete, the virus will utilize the VLDL pathway and be secreted outside the cell where it can infect other hepatocytes (Fig. 1) (48).

1.2.1 Hepatitis C Virus Proteins and Functions

The viral polypeptide which is produced by host ribosomes is 3,000 amino acids long, and is cleaved into ten separate proteins by both viral and host proteases (Fig. 2). These proteins include core, E1, E2, p7 ion channel, NS2, NS3, NS4A, NS4B, NS5A, and NS5B. The three structural proteins, core, E1, and E2 are cleaved by endogenous proteases whereas the non-structural proteins are cleaved by the viral proteases NS2-3 autoprotease and NS3-4A serine protease (42, 46). The individual proteins will then attach to the ER membrane, and viral replication will ensue. E1 and E2 glycoproteins form non-covalent heterodimers stabilized by disulfide bonds, and are vital for viral entry (77, 97). These glycoproteins are glycosylated on their N-terminal ectodomain which is necessary for correct protein folding, attachment to proper receptors during viral entry, as well as masking the virus from an immune response which could stimulate neutralizing antibody production (40, 44). Core is a protein with dual domains (19). Core D1 is a hydrophilic domain which may bind RNA during virion production, and core D2 is what binds the ER outer membrane (90). Core D2 also allows the protein to associate with lipid droplets, which is believed to be a factor during viral assembly (9, 63, 72).

The two HCV proteins which are not utilized for genomic replication, but are necessary for infectious virus are the p7 ion channel and NS2 non-structural protein. The p7 ion channel is a protein with two transmembrane domains, and is classified as a viroporin. Both cell culture and *in vivo* models have shown that p7 is involved in assembly and release of viral particles (52, 89, 91). Studies showed that p7 is not involved in viral entry, but during the late phase of viral assembly. NS2 recently has also been reported to be involved in viral assembly. It is thought that in addition to having autoprotease activity, it may also connect the structural and non-structural proteins during viral assembly (84).

The rest of the non-structural proteins are involved in the viral genomic replication complex. In addition to being a serine protease in conjunction with NS4A, NS3 also acts as a helicase which is necessary for replication (60). The helicase activity is required during an early step of viral particle formation. NS4B stimulates formation of the membranous web needed for viral replication (41, 79). The membranous web was first shown to harbor RNA replication while studying the viral lifecycle in Huh7 cells. NS4B is also needed in viral assembly. One group showed that when NS4B was mutated, membranous web formation ceased to occur along with viral particle formation (53). However when the replicons were reconstituted with intact NS4B, particle formation ensued. The NS5A protein is involved in both RNA replication and viral particle formation (8, 93). This protein contains three domains which each have different functions. Domains I and II are involved in replication, whereas III is involved in assembly (8). The last protein, NS5B, is an RNA-dependent RNA polymerase (22). NS5B's C-terminal end is embedded in the ER membrane, while the N terminal side performs the RdRp reaction along with certain host factors (71).

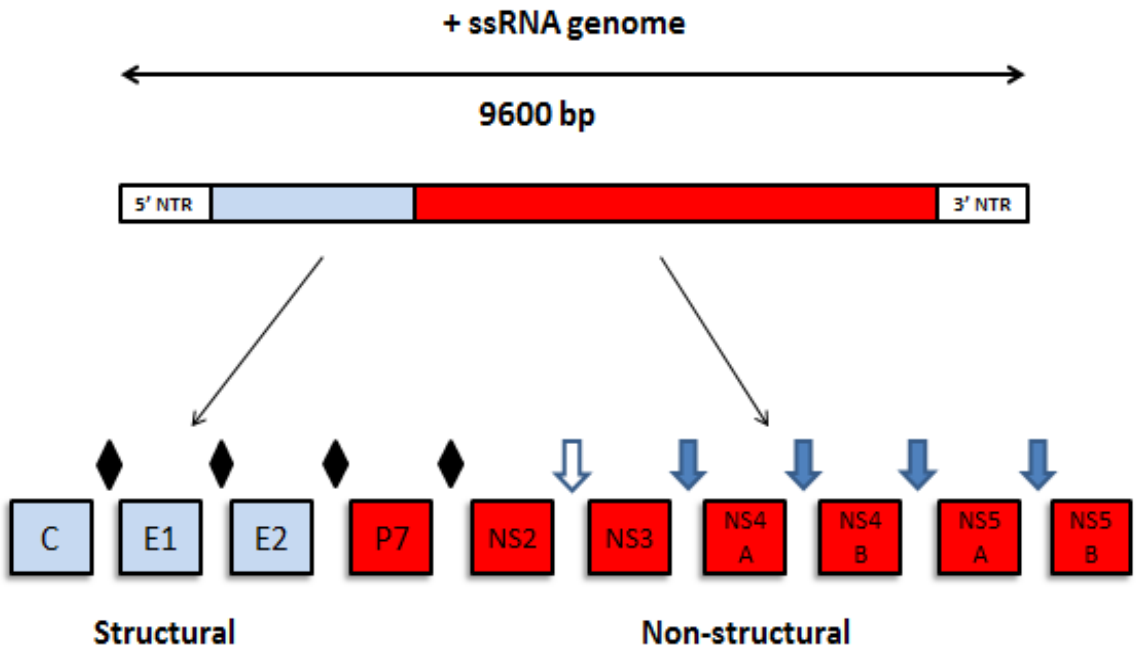

Figure 2. Hepatitis C virus genome and proteins. The 9,600 base pair genome is translated into a 3,000 amino acid long polypeptide, which gets cleaved into 10 viral proteins. Host ER signal peptidases will cleave the structural proteins (black diamonds), and the non-structural proteins will be cleaved by a combination of the viral NS2-3 protease (white arrow), and the NS3-4A protease (blue arrows).

1.2.2 Apolipoprotein E and Hepatitis C Virus

Apolipoprotein E (ApoE) is a 299 amino acid long polypeptide synthesized in hepatic parenchymal cells and normally functions in the transport of lipids within the body (62). It can associate with cholymicrons, VLDL, and HDL. Apo E has multiple receptors including low density lipoprotein receptor (LDLR), very low density lipoprotein receptor (VLDLR), apolipoprotein E receptor 2 (apoER2), and heparan sulfate proteoglycan (HSPG) (20, 45). ApoE contains a LDLR binding region in the N terminal domain. This binding region resides within a four-helix-bundle between amino acids 136-150. Within the C terminal domain is the major lipid-binding region between amino acids 245-266. When ApoE is bound to a phospholipid, it will adopt an α-helical hairpin like structure based on EPR, FRET, and X-ray diffraction studies (31, 43, 76).

It has been shown that HCV is in association with lipoproteins apoE and apoB (6, 7, 21). Scientists were puzzled for many years as to why patient-isolated HCV had different densities and sedimentation rates, and the answer was because the virus associates with host derived very low-density lipoproteins (VLDL) containing apo E and apo B (37, 87). HCV production is closely tied to VLDL production. In a cell culture model, apoE-specific monoclonal antibodies neutralized HCV infectivity in a dose dependent manner (21). At the same time, siRNA knockdowns of apoE expression in cells reduced intracellular as well as secreted HCV. These findings demonstrated that apoE is necessary for both HCV entry and exit. The fact that HCV uses hepatocytes for infection and assembly makes sense since they are the primary producers of lipoproteins in the body, as well as the organ where cholesterols get transported for degradation (62). When analyzing how HCV interacts with apo E, it was shown that the NS5A protein interacts with the C-terminal alpha helix of apo E (16, 30). Without the ability of NS5A to interact with apo E, HCV would not be infectious.

In addition to apo E and apo B, mass spectrometry analysis has recently shown that HCV is in association with the lipids cholesterol, cholesterol esters, phosphatidylcholine, and sphingomyelin (66). Cholesterol and sphingomyelin were first shown to be important in viral infectivity after a group demonstrated that HCVcc became less infectious after removing these two lipids (3). HCVcc was first treated with methyl- β-cyclodextrin (B-CD) which can remove cholesterol from membranes (82). When treated in a dose-dependent manner with increasing concentrations of B-CD, the virus became less infectious (3). 5 mg/mL of B-CD reduced core protein levels in Huh-7 by 98% compared to untreated virus. Infectivity of the virus was restored after removal of the B-CD and reconstitution of cholesterol. At the same time, removal of sphingomyelin with increasing concentrations of the enzyme SMase lead to dose-dependent

viral infectivity loss (3). 1 U/mL of SMase led to 90% reduction in infectivity compared to the untreated.

1.2.3 Hepatitis C Virus Entry into Human Hepatocytes

There are two particular viruses that are used to study hepatitis C entry and its lifecycle. These are the hepatitis C pseudoparticle (HCVpp), and hepatitis C cell culture (HCVcc). HCVpp is lentiviral based and is used to study viral entry (12). It contains the lentiviral gag and pol in its genome as well as a reporter gene. The envelope is studded with the hepatitis C glycoproteins E1 and E2. HCVpp can only be used to study viral entry. In 2005, the first infectious cell culture based hepatitis C virus was introduced. HCVcc was derived from JFH-1 subtype 2a, and was the first hepatitis C virus to complete its lifecycle *in vitro* (56, 99) (Fig. 3). When a full

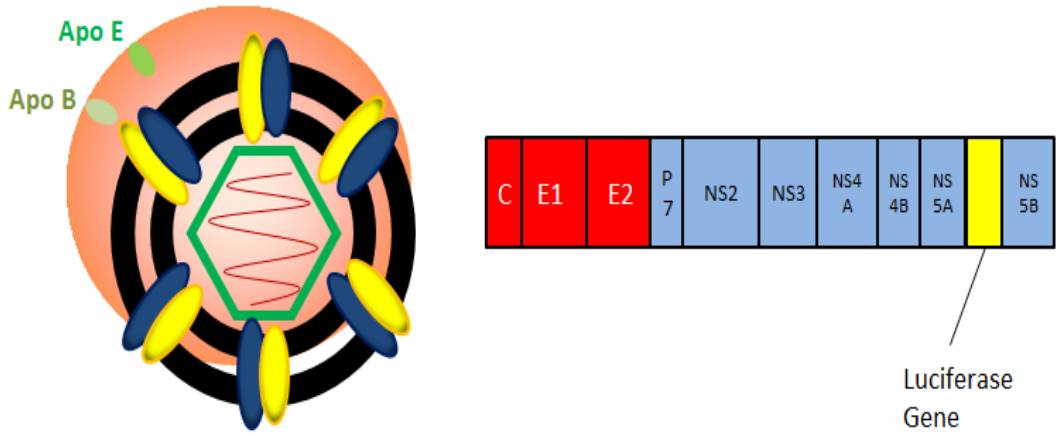

Figure 3. HCVcc design. HCVcc contains the full length viral genome, with a luciferase gene inserted in between the NS5A and NS5B genes. It is an authentic HCV particle that is able to complete its lifecycle in cell culture.

length JFH-1 RNA strand was transfected into Huh7 cells, it resulted in the secretion of infectious HCVcc particles. Later on, a reporter gene was added. This infectious clone was a

breakthrough in the field as researchers could better observe how and where the virus enters, replicates, and exits.

Much work has been done in order to elucidate how HCV enters hepatocytes, and what host factors are needed. The glycosaminoglycan heparan sulfate (HSPG) was recognized as an initial binding factor needed to attach the virus to the cell surface of hepatocytes (10, 11). The E2 glycoprotein was shown to be involved in attachment to HSPG. Once the virus binds heparan sulfate, it will then attach to the other necessary receptors. When HCVcc and HCVpp were pretreated with heparin, a homologue of heparan sulfate, viral infection was inhibited (14). However, if the virus was added before the addition of heparin, there were no inhibitory effects on viral infectivity. A recent publication has shown strong evidence that apo E also is involved in attaching the virus to HSPG (51). Even when an E2 specific monoclonal antibody was added, HCV attachment still occurred. These studies demonstrate that heparan sulfate is needed for early binding by HCV, but not during the late stage of viral entry.

The low-density lipoprotein receptor (LDLR) is now considered an HCV entry receptor. This was first proposed after HCV was shown to be in association with LDL and VLDL (2). Later, one group showed that when COS-7 cells were transfected with a vector allowing them to express LDLR, HCV positive sera tested on these cells resulted in binding of viral particles in 7 out of 12 patient samples (70). The same group showed that the addition of >200 μg/ml of pure low density lipoproteins to human fibroblasts expressing LDLR inhibited HCV binding. They proposed that the LDL added was in competition with HCV for binding to the LDLR. It was also shown that monoclonal antibodies which targeted the LDLR as well as apoE and apoB inhibited infection of primary human hepatocytes (2, 38). When the LDLR monoclonal antibodies were added at the same time as the virus, infection was inhibited. When the antibody

was added at later time points following the addition of the virus to cells, it was not effective in blocking infection. Therefore, the conclusions are that LDLR is involved in an early step in viral entry (69). Together both heparan sulfate and LDLR are binding factors which are used by HCV for initial attachment.

CD81 is a receptor which is part of the tetraspanin family of proteins. It was the first discovered entry factor for HCV (5, 13, 34, 81). This protein spans the membrane four times, forming two extracellular loops: a long extracellular loop (LEL) and a short extracellular loop. The long extracellular loop (LEL) is what interacts with the E2 glycoprotein allowing viral entry (34). Previous studies showed that soluble E2 could bind to CD81, and that four cysteines in the LEL are needed for efficient binding (80). Once HCVpp and HCVcc were developed, experiments were done in which these viruses were pretreated with the LEL of CD81. This inhibited viral infectivity of Huh7 cells (4, 17, 73). Antibodies against CD81 also inhibited viral entry into Huh7 cells when added prior to the addition of HCVcc, or after the binding step at 4° C (28, 54). HepG2 cells, which is a human heptoma cell line lacking CD81, is naturally resistant to hepatitis C infection. Once these cells were transfected with DNA encoding CD81, they became susceptible to infection by HCVpp, but not to the same magnitude as Huh7 cells (34).

A highly expressed protein on the liver which has also been shown to be necessary for HCV infection is the scavenger receptor class B, member 1 (SRB1). This protein crosses the plasma membrane twice forming an extracellular loop. Its primarily function is as an HDL receptor and is important in cholesterol transport (1, 27, 49). In regards to HCV, SRB1 was shown to be an entry factor when expressed in 293T cells. 293T cells which were overexpressed with SRB1 had a 10 fold increase in viral infection with HCVpp compared to cells which did not express SRB1 (13). Also, anti-serum against SRB1 reduced infectivity in Huh7 cells

significantly. An interesting finding in regards to SRB1 is that HDL uptake increased HCVpp infectivity. When HDL was added to cells after the binding of HCVpp, there was a 5-fold increase in infectivity compared to when HDL was added with the virus at the same time (98). These results led to the speculation that HDL aids HCVpp infection at a post binding step.

One of the entry factors that was discovered to be involved during the later stage of hepatitis C virus entry was claudin-1. This is a tetraspan transmembrane protein involved in forming tight junctions creating a paracellular seal (35, 74). Paracellular sealing is important for epithelial and endothelial cells so they can maintain polarity as well as control the passage of solutes and ions through the space between cells. Altogether, claudin-1 forms two extracellular loops, and one intracellular loop (35, 36). Claudin-1 is highly expressed on the liver, and on many endothelial cells. It was first discovered as a receptor for HCV when a cDNA library derived from a permissive cell line was expressed in 293T cells which contained CD81 and SRB1 (32). This expression caused the cells to become susceptible to hepatitis C virus entry. Further evidence showed that when siRNA was used to knockdown claudin-1 in permissive cells, HCVcc and HCVpp had decreased infectivity (32, 64). It was next determined that the N-terminal 1/3 of extracellular loop 1 (ECL1) was necessary for viral infection, demonstrated by changing two residues in the ECL1 of claudin-7 to that of claudin-1. The ECL1 change in claudin-7 allowed 293T cells to become susceptible to HCVpp infection (30). Investigators who were studying claudin-1, showed that it acts in a post-binding step, and believed that CD81 binding by HCV needed to occur before the virus could bind to claudin-1 (32, 64). Antibody inhibition studies demonstrated the function of CD81 in HCV infection. When an anti-CD81 antibody was added to 293T cells prior to the addition of HCVpp, infection of the virus was

inhibited. Also, when Hep-G2 (CD81 deficient) cells were overexpressed with claudin-1, HCVpp infection still did not occur.

The most recently identified receptor which has been recognized in HCV entry is occludin (15). Occludin is a four transmembrane protein which is also involved in tight junction formation. Our lab was the first to show that when siRNA was used to knockdown occludin in susceptible cells, it inhibited viral infection of HCVcc and HCVpp (59). In analyzing when occludin comes into play during HCV entry, it was determined to be involved at a post-binding step after co-immunoprecipitation studies showed interaction between HCV E2 glycoprotein and occludin (15). Specifically, the second extracellular loop was shown to be important in viral

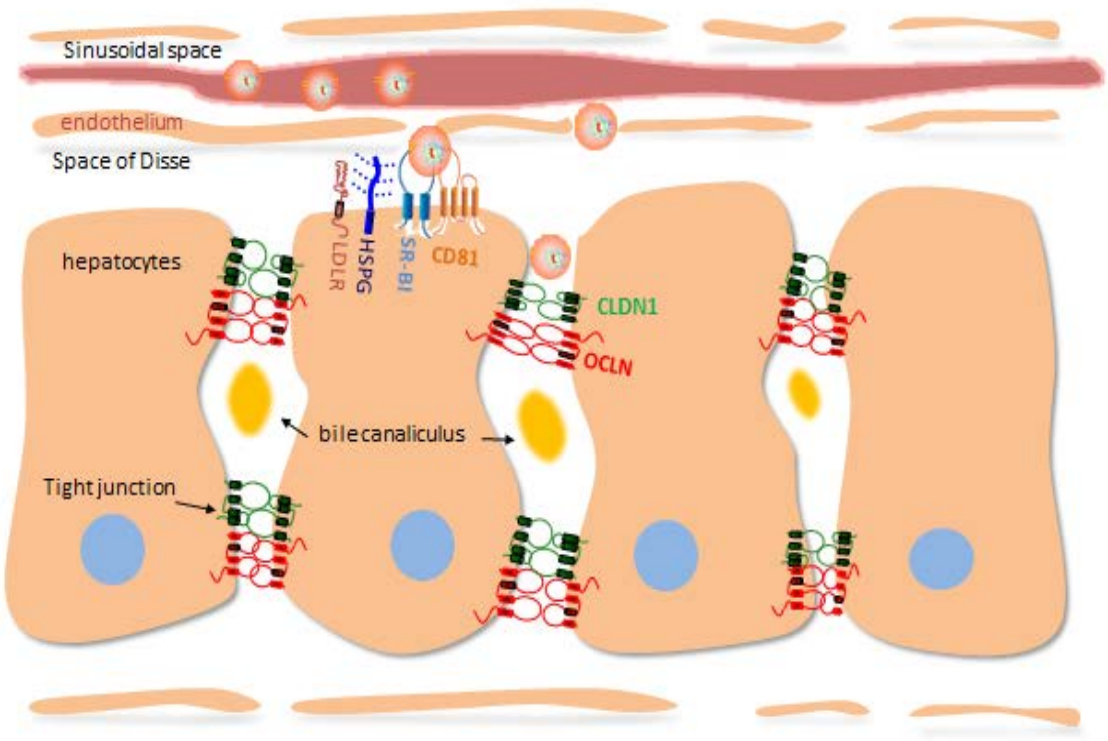

Figure 4. Hepatitis C virus entry into human hepatocytes. HCV will utilize the known binding factors/receptors to gain entry into hepatocytes: LDLR, HSPG, SR-B1, CD81, claudin-1, and occludin.

entry, as its removal inhibited HCVpp infectivity (57). Occludin was also shown to be important in species specificity. The addition of human CD81 and occludin made mouse cells susceptible to HCV infection (83). Another finding in our lab was that dynamin II interacts with the second extracellular loop of occludin and is important for HCVpp and HCVcc entry into cells (57). Dynamin II is a GTPase which has been shown to be necessary for internalization of clathrin-coated vesicles, and since HCV enters cells via clathrin-mediated endocytosis, dynamin II may be necessary for HCV entry (86). With these findings, our lab concluded that the binding of HCV to the second extracellular loop of occludin, may dictate HCV dynamin-dependent endocytosis into cells.

1.2.4 Human Apolipoprotein E Peptide

The anti-HCV effects of the human apolipoprotein E peptide were a major finding by our lab. This peptide was designed based on the rationale that by combining the lipid binding and receptor binding regions of apo E (Fig. 5A), a peptide would be created which could outcompete HCV associated apo E for binding to cellular receptors (58). When tested in cell culture on Huh7.5.1 cells, hEP had an IC_{50} of 0.67 μM (Fig. 5B), and showed no signs of cytotoxicity even when 14 μM was tested (Fig. 5C). As a comparison, mouse apolipoprotein E peptide was created. This peptide did not express the same inhibitory effects as hEP. Another benefit of hEP is that it is a stable peptide, as it was able to retain its anti-HCV effects in cell culture for up to 24 hours. However, its anti-HCV effects were shown to diminish at 48 hours.

In addition to being a potent inhibitor of HCVcc, hEP was also shown to bind lipids *in vitro* and lower plasma cholesterol levels in mice (58). In a cell culture model, dimyristoylphosphatidylcholine (DMPC) liposome vesicles were added in the presence of hEP or

mEP, and it was discovered that the peptides were able to bind to the DMPC particles as well as to the LDLR. When injected into mice, both hEP and mEP were able to lower plasma cholesterol levels to the same degree. This finding showed that hEP has dual functions, as it can inhibit HCV entry into cells as well as bind lipids.

The intact LDLR region of hEP is crucial for blocking HCV entry. Twelve different hEP molecules were synthesized, but only hEP 1 and hEP 2 had intact LDLR regions (58). hEP 1 contained both the LDLR and lipid binding regions, whereas hEP 2 only had the LDLR region with a cysteine residue added on the N terminal side to give the peptide greater stability and the ability to dimerize. The added cysteine proved to be important for the function of hEP 2, as hEP 2/ΔCys resulted in failure to inhibit HCV infection. hEP 3 contained only the lipid binding region with a cysteine residue added at the N terminal side, and it failed to inhibit infection as well. The rest of the hEP molecules (hEP 4-12) were either truncated versions of the LDLR, the lipid binding region, or a combination of both. None of these peptides inhibited HCV infection to the same degree as hEP 1 or 2. hEP 2 was shown to be the ideal sequence for inhibiting HCV infection.

Further analysis of hEP showed that it specifically blocked HCV binding to cells (58). During a time-of-addition experiment, hEP was added to Huh7.5.1 cells together with HCVcc at 4°C attachment step, or added during the transfer of the cells and virus to 37°C. When added after the temperature shift, hEP exhibited little inhibition demonstrating that it inhibits viral entry during the attachment stage. hEP does not decrease the levels of potential HCV receptors on cells. This was determined after treating cells with hEP, and using flow cytometry to analyze if all the necessary receptors were still present. Even though hEP was able to block HCVcc entry, it was not able to block HCVpp entry. 293T cells are used to produce HCVpp, and these cells do

not produce apo E. Therefore the virus does not associate with apo E and is not needed for entry into susceptible cells. hEP did however block patient serum-derived HCV viral entry into primary human hepatocytes (PHH). The overall conclusion on hEP is that it blocks HCV at the initial binding step. It is not known whether it individually binds both LDLR and HSPG, or even both together. Regardless, initial binding is blocked and this peptide outcompetes virion associated apo E for the binding to its receptors.

2.0 STATEMENT OF THE PROJECT

The effects of the hEP peptide showed that it could not only inhibit HCV entry in cell culture at sub-micromolar concentrations, but it could also lower plasma cholesterol levels as well as suppress inflammation in mice (58). This is why hEP looks to be a promising therapeutic. After the production of hEP, we realized that it is a very expensive peptide to produce because it is synthetically made. Also, it is a peptide with a short half-life, as its anti-viral effects were diminished after 48 hours. Therefore we sought to develop an hEP which would have a longer half-life in addition to being cheaper to produce. We felt the best way to increase the half-life of hEP was to fuse it to human serum albumin (HSA). HSA is the most abundant protein in the body, and has a long natural half-life which allows it to maintain oncotic pressure (26). The rationale for fusing hEP to HSA was based on the findings of another group which fused IFN-α to HSA: termed Albuferon. Albuferon was shown to have increased pharmacokinetics, a longer half-life, and a slower rate of clearance over standard IFN-α (78). We predicted that the same would be true for hEP by fusing it to HSA. In order to produce this fusion protein, we used the methylotropic yeast strain X-33 *Pichia pastoris* because it is a eukaryotic system which can secrete heterologous recombinant protein with the appropriate post-translation modifications in large quantities (29). If we are able to produce the hEP and HSA fusion protein in large quantities using X-33 *Pichia pastoris* and show that hEP has the same

effects with a longer half-life, then this will be a cheaper method to produce a more effective therapeutic. To test this hypothesis, our objectives were:

Aim 1: To construct human apolipoprotein E peptide and human serum albumin fusion plasmids as well as X-33 *Pichia pastoris* clones

Aim 2: Produce the recombinant proteins of interest, and test the anti-HCV effects in cell culture using Huh7.5.1 cells and HCVcc-luciferase

3.0 MATERIALS AND METHODS

3.1 CONSTRUCTION OF HUMAN APOLIPOPROTEIN E PEPTIDE AND HUMAN SERUM ALBUMIN FUSION PLASMIDS AS WELL AS X-33 *PICHIA PASTORIS* CLONES

3.1.1 Subcloning into pPICZαA

The plasmid pPICZαA was purchased from Invitrogen and expanded in DH5α E. coli cells. Sequence specific primers for human serum albumin, hEP, and mEP were designed with specific restriction enzyme recognition sites (Table 1). The plasmid already contained a coding region for a 6X histidine tag (Fig. 5A) After the appropriate PCR materials were added (Table 2), the insert DNA was amplified by PCR using a Bio-Rad MJ thermocycler (Table 3), and then purified using a PureLink PCR purification kit from Invitrogen. Once the DNA had been amplified and purified, it was then double digested with the appropriate restriction enzymes (Table 4). The digested DNA was purified by running it on a 0.8% agarose gel and extracted using an Omega gel extraction kit. The inserts were ligated into pPICZαA using T4 DNA ligase purchased from New England Biolabs (Table 5). The ligation took place for 2 hours at room temperature. The ligated plasmid was transformed into Top 10 E. Coli cells. Plasmid DNA was isolated using an Omega midi prep kit. 1 µg of the extracted DNA was double digested for 1

hour with EcoR1 and Kpn1 for confirmation that the inserts had ligated into the vector. The double digest was run on a 0.8% agarose gel, and if the two bands of the appropriate size were present, then the plasmid was sent for Sanger sequencing.

Table 1. Sequence specific primers.

Primers	Sequence	
Human Serum Albumin:	Forward	GCGCGAATTCATGAAGTGGGTAACCTTTATTTCC
	Reverse	CGCGGGTACCTAAGCCTAAGGCAGCTTGACTTGCA
Human Serum Albumin (N):	Forward	GCGCGAATTCATGAAGTGGGTAACCTTTATTTCC
	Reverse	CGCGACTAGTTAAGCCTAAGGCAGCTTGACTTGCA
Human Serum Albumin (C):	Forward	AGACTAGT GGCGGCGGCGGCGGCGGCAAGTGGGTAACCTTTATTTC
	Reverse	CGCGGGTACCTAAGCCTAAGGCAGCTTGACTTGCA
hEP (N):	Forward	AGGAATTCGAAGAACTGCGTGTTCGTCT
	Reverse	AGACTAGTCATGTCTTCAACCAGAGGCT
hEP (C):	Forward	AGACTAGTGGCGGCGGCGGCGGCGGCGAAGAACTGCGTGTTCGTCT
	Reverse	GAGGTACCCACATGTCTTCAACCAGAGGCT
mEP (N):	Forward	AGGAATTCGAAGAAATCCGTGCGCGTCT
	Reverse	AGACTAGTCATGTCTTCAACGATCGGTT
mEP (C):	Forward	AGACTAGTGGCGGCGGCGGCGGCGGCGAAGAAATCCGTGCGCGTCT
	Reverse	GAGGTACCCACATGTCTTCAACGATCGGTT

Table 2. PCR reaction mixture contents

PCR Reaction Mixture	Amount
5X Phusion buffer	10.0 µL
10 mM dNTP	1.0 µL
10 mM forward primer	2.5 µL
10 mM reverse primer	2.5 µL
Template DNA	1.0 µL
Phusion polymerase	0.5 µL
Water	32.5 µL
Total	50.0 µL

Table 3. PCR conditions

Cycle Step	Temperature	Time	
Initial Denaturation	98° C	30 seconds	
Denaturation	98° C	10 seconds	
Annealing	55° C	30 seconds	35 cycle
Extension	72° C	30 seconds	
Final Extension	72° C	10 minutes	
Forever	4° C		

Table 4. Double digestion reactions

pPICZαA	Amount	**Human Serum Albumin only**	Amount	**N terminal inserts**	Amount	**C terminal inserts**	Amount
DNA	1 µL	DNA	5 µL	DNA	10 µL	DNA	10 µL
EcoR1	1 µL	EcoR1	1 µL	EcoR1	1 µL	Spe1	1 µL
Kpn1	1 µL	Kpn1	1 µL	Spe1	1 µL	Kpn1	1 µL
EcoR1 buffer	5 µL	EcoR1 buffer	5 µL	NEB buffer 1	5 µL	NEB buffer 1	5 µL
BSA	0.5 µL	BSA	0.5 µL	BSA	0.5 µL	BSA	0.5 µL
Water	41.5 µL	Water	37.5 µL	Water	32.5 µL	Water	32.5 µL
Total	**50.0 µL**	**Total**	**50.0 µL**	**Total**	**50.0 µL**	**Total**	**50.0 µL**

Table 5. Ligation reactions

Human Serum Albumin only	Amount	N terminal and C terminal insert	Amount
pPICZαA	1 µL	pPICZαA	1 µL
HSA insert	10 µL	N terminal insert	3 µL
T4 DNA Ligase buffer	2 µL	C terminal insert	3 µL
T4 DNA ligase	1 µL	T4 DNA buffer	2 µL
Water	5 µL	T4 DNA ligase	1 µL
Total	20 µL	Water	10 µL
		Total	20 µL

3.1.2 Propagation, Electroporation, and Purification of X-33 *Pichia Pastoris*

X-33 *Pichia pastoris* was purchased from Invitrogen, and streaked on a yeast, peptone, dextrose (YPD) plate and incubated at 30º C for 2 days. Two days prior to electroporation, a yeast colony was picked and used to inoculate 5 mL of YPD media, and shaken overnight at 30º C, 300 rpm. The following day, the 5 mL culture was used to inoculate 250 mL of YPD in a 1,000 mL flask and shaken overnight at 30º C, 300 rpm. Once the OD_{600} reached 1.3, the cells were spun down, and initially resuspended in 250 mL of water, and then in 1 M sorbitol to a final volume of 1.5 mL. 10 µg of linearized plasmid DNA containing the appropriate insert was linearized and mixed with 80 µL of cells in a 0.3 mm ice cold BioRad electroporation cuvette. A Bio-Rad Gene Pulser was used to electroporate the yeast cells on the settings: 1,500 V, 25 µF capacitance, 200 Ω resistance. Immediately after electroporation, 1 mL of 1 M sorbitol was added to the cuvette and the contents were transferred to a 15 mL tube and incubated at 30º C for 2 hours. Different volumes (25 µL, 50 µL, 100 µL, 200 µL) of electroporated cells were then spread on 100 µg/mL yeast, peptone, dextrose, sorbitol (YPDS) zeocin plates and incubated at 30º C for 3 days. Once colonies grew, 6-10 were picked and streaked on 100 µg/mL YPDS zeocin plates for purification. The streaked colonies were further purified by being streaked on 500 µg/mL YPDS zeocin plates.

3.1.3 *Pichia pastoris* Colony PCR

Pichia pastoris colonies which were streaked on 500 µg/mL zeocin YPDS plates were tested to determine whether or not they contained the linearized electroporated plasmid DNA within their genome. All streaked colonies had a small portion picked with a pipette tip and

added to a PCR tube containing 2 µL of water. The integrated plasmid contains two AOX1 primer regions which are used for detecting the subcloned fragment. These regions are referred to as the AOX1 forward (F) region, and the AOX1 reverse (R) region. Depending on the construct being tested, either an AOX1 F primer or AOX1 R primer was used along with a sequence specific primer for hEP, mEP, or HSA. Each individual PCR tube contained 16.875 µL of deionized water, 5µL of 5X Go Taq Buffer, 0.5 µL of 10 mM dNTP's, 0.25 µL of 100 mM forward primer, 0.25 µL of 100 mM reverse primer, 0.125 µL of Go Taq polymerase.

3.2 PRODUCTION OF RECOMBINANT PROTIENS OF INTEREST AND TESTING OF ANTI-HCV EFFECTS IN CELL CULTURE

3.2.1 Recombinant Protein Production

Individual colonies electroporated with a different plasmid construct were picked and used to inoculate 25 mL of buffered complex medium containing glycerol (BMGY: 1% yeast extract, 2% peptone, 100 mM potassium phosphate: pH 6.0, 1.34% Y NB, 4x10-5 biotin, 1% glycerol) in a 250 mL flask, shaking at 30º C, 300 rpm. These flasks were shaken for 26-28 hours until the OD_{600} was 2 or higher. 700 µL of the culture was removed and mixed with 300 µL of 50% glycerol in a cryogenic tube. These tubes were stored at -80º C for long term storage. The rest of the cultures were then spun down at 1,500 rpm for 5 minutes, and the supernatant was poured out. The pellet was then washed with 20 mL of buffered complex media containing methanol (BMMY: 1% yeast extract, 2% peptone, 100 mM potassium phosphate: pH 6.0, 1.34%

YNB, 4x10-5 biotin, 0.5% methanol) in order to remove any leftover glycerol. The cells were then spun down again and resuspended in 200 mL BMMY. The transfer of the cells from BMGY to BMMY is what induced recombinant protein production, as methanol being the sole carbon source stimulated translation from the AOX1 promoter located in the integrated plasmid. The cultures were shaken at 30º C, 300 rpm. Every twelve hours, methanol was added to the cultures to a final concentration of 3%. After 48 hours, the cultures were spun down and the supernatant was separated from the pellets, and both were stored at -80º C.

3.2.2 Lysis of *Pichia pastoris* Pellets

Pellets were collected from -80°C and thawed on ice. 15 mL of breaking buffer (BB: 50 mM sodium phosphate pH 7.4, 1mM PMSF, 1 mM EDTA, 5% glycerol) along with a volume 5 mL of 0.35 µm acid washed beads were added. The pellets were then vortexed for 1 minute, and then put on ice for 1 minute for eight total cycles. The lysate was then spun at 4,700 rpm for 10 minutes at room temperature. The supernatant was then collected and analyzed for recombinant protein presence by Western blot.

3.2.3 Western Blot Assay

Cell lysates were separated by gel electrophoresis in 8% sodium dodecyl sulfate (SDS)-polyacrylamide gel and proteins were transferred to a nitrocellulose membrane using the Mini Trans-Blot electrophoretic transfer cell (Bio-Rad) in transfer buffer (15.6 mM Tris base, 120 mM glycine). The membrane was then blocked with 10% skim milk in wash buffer for 45 minutes at room temperature. The membranes were then incubated overnight at 4º C or for two hours at

room temperature with a rabbit anti-histidine polyclonal antibody in 5% milk in wash buffer at a 1:5000 dilution. The membranes incubated with this primary polyclonal antibody were incubated with horseradish peroxidase-conjugated goat anti-rabbit IgG in 5% milk in wash buffer at a 1:1000 dilution for 1 hour at room temperature. The signal was visualized by chemiluminesence by the addition of ECL substrate solution. Films were exposed for either 1, 5, or 30 seconds.

3.2.4 Recombinant Protein Isolation

Batch purification was performed on all the cell lysates. 5 mL of lysate was mixed with 5 mL of PBS and mixed with 150 µL of PerfectPro Ni-NTA agarose beads in a 15 mL tube. Prior to the addition of the lysate mixture to the beads, the beads were washed with 5 mL of breaking buffer. After the wash, the lysate mixture and beads were rotated at 4° C for two hours. The lysate was then removed and the beads were rinsed with 5 mL of PBS to remove background proteins. The beads were then mixed with 1 mL of 200 m M imidazole in order to elute the bound recombinant protein. After the imidazole was collected, the beads were then boiled in 2X sample buffer to elute off any remaining protein. This was performed to see whether the imidazole had eluted off the bound protein

3.2.5 Protein Quantification

A BCA assay protein quantification kit was purchased from Thermo Fisher, and used to quantify the total protein in each cell lysate. Recombinant protein quantification was performed by loading different amounts of a His-tagged protein with a known concentration on an 8% SDS

gel, and then comparing the intensity of the recombinant protein bands to the known protein standard. From there, a concentration of recombinant protein could be calculated.

3.2.6 Protein Concentration

Lysates were concentrated by adding 5 mL to an Amicon Ultra-15, PLTK Ultracel-PL Membrane, 30 kDa centrifugal device, and then spinning at 3,000 rpm until the lysate level was at 500 µL. The 500 µL of lysate was then diluted in 10 mL of PBS and then spun down again to a volume of 500 µL. This was performed in order to remove the salts in the breaking buffer, and make the lysates as isotonic as possible. All recombinant proteins of interest were greater than 30 kDa in size.

3.2.7 Cell Lines and Reagents

The Huh7.5.1 line was provided by Dr. Francis Chisari (Scripps Research Institute). This cell line was maintained in DMEM supplemented with 5% Penicillin and streptomycin, 1% NEAA and 10% fetal bovine serum (FBS) (Gemini Bio-Products).

3.2.8 Infectivity Assay

Huh7.5.1 cells ($1x10^4$) were plated in a 48 well plate and grown to 80% confluency. Different volumes of yeast lysates containing the recombinant proteins of interest were added in duplicate to the wells, along with 180 µL of HCVcc luciferase and 120 µL of DMEM. The lysate and virus incubations occurred for three hours before they were removed. After the

removal, the cells were rinsed with 200 µL of DMEM and then had 300 µL of fresh DMEM added. After 48 hours, the cells were lysed with 50 µL of 5X passive lysis buffer diluted to 1X in PBS. They were then gently rocked for 15 minutes on an orbital shaker, after which 50 µL of the lysate was mixed with 50 µL of luciferase assay reagent II (LARII) in a 96 well luminometer plate. The mixture was quickly added to a Veritas luminometer where a luciferase reading ensued. Each experiment contained two wells to serve as a negative control (uninfected and untreated cells), and two wells to serve as a positive control (infected and untreated cells).

3.2.9 Cell Viability Assay

Huh7.5.1 cells ($1x10^4$) were plated in a 48 well plate and grown to 80% confluency. Different volumes of X-33 *Pichia pastoris* lysate were added in duplicate to the wells. DMEM was then added so that the final volume in each well was 200 µL. The lysate/DMEM mixture was allowed to incubate with the cells for three hours, after which it was removed and replaced with fresh DMEM. After 48 hours, the cells were lysed with 5X passive lysis buffer diluted to 1X in PBS, and 50 µL of lysate was mixed with 50 µL of cytopathic effect (CPE) luciferase reagent. This reagent consisted of 1ml of a 5X D-Luciferin Stock Solution (1 mM D-luciferin, 25 mM Glycylglycine, 10 mM DTT), 1 ml luciferase enzyme (1 mg/ml), 0.5 ml 250 mM Glycylglycine and 3.5 ml water in 9 ml Luciferase Assay Buffer (25mM Glycylglycine pH 7.8, 15 mM Potassium Phosphate pH 7.8, 15mM MgSO4, 4mM EGTA in H2O). The lysate/CPE reagent mixture was added to a 96 well luminometer plate and inserted into a Veritas luminometer to measure luciferase activity.

3.2.10 Imnunofluoresence Staining and Confocal Microscopy

Huh7.5.1 cells were plated to 90% confluency in a 24 well plate which contained glass coverslips. 48 hours after the cells were treated, they were then washed with 1X PBS, and fixed with 2% paraformaldehyde (15 min, RT). After a second wash with 1X PBS, the cells were permeablized with 0.1% Triton X-100 in PBS (15 min, RT). A wash with 1X PBS and PBB (PBS+ 0.5% BSA) followed, and then blocking with 2% BSA for 45 minutes. After this time period, primary antibodies against core protein and E2 glycoprotein were diluted in PBB and 100 µL of the mixture were added to the cells and incubated for 1 hour. Following a wash with PBB, the secondary antibodies Alexa Fluor 568 (Red) and Alexa Fluor 488 (Green) were added. Alexa Fluor 568 was against E2 and Alexa Fluor 488 was against core. The secondary antibodies incubated for 1 hour. The nucleus was stained with Draq5, after which the cells were washed with PBB and Hoescht stained for 30 seconds. After a final wash, the coverslips was adhered slides using gelvatol. The slides were then taken to the University of Pittsburgh Center for Biological Imaging. Images were captured on a Carl Zeiss Meta LSM 510 confocal microscope.

4.0 RESULTS

4.1 SPECIFIC AIM 1 RESULTS

Aim 1: To construct human apolipoprotein E peptide and human serum albumin fusion plasmids as well as X-33 *Pichia pastoris* clones

4.1.1 Subcloning into pPICZαA

The plasmid pPICZαA was used because it contains an alpha secretion factor derived from *Saccharomyces cerevisiae*, as well as an AOX1 promoter which is activated in the presence of methanol (Fig. 5A). Additionally, it contains a zeocin resistance gene and a c-myc epitope along with a (6X) polyhistidine tag. Within the alpha secretion signal gene is a region harboring a Kex2 cleavage site as well as a Ste13 cleavage site. Once the fusion protein is produced, host proteases will cleave the alpha secretion signal off before secretion, leaving only the protein of interest and the c-myc/polyhistidine tag. The first gene which was subcloned into this pPICZαA was HSA (Fig. 5B). It was subcloned in frame with the alpha secretion factor, c-myc epitope, and (6X) polyhistidine tag. This construct, pPICZαA HSA, was used to produce recombinant protein which served as a negative control during the cell culture work. hEP and mEP were subcloned into pPICZαA with HSA. Both hEP and mEP were fused to the C terminal side of HSA, creating pPICZαA HSA-hEP, and pPICZαA HSA-mEP (Fig. 6A). Separating the two

inserts was a (6X) glycine polylinker which was engineered to give flexibility to the fusion protein once it was produced. hEP and mEP were also subcloned into the vector on the N

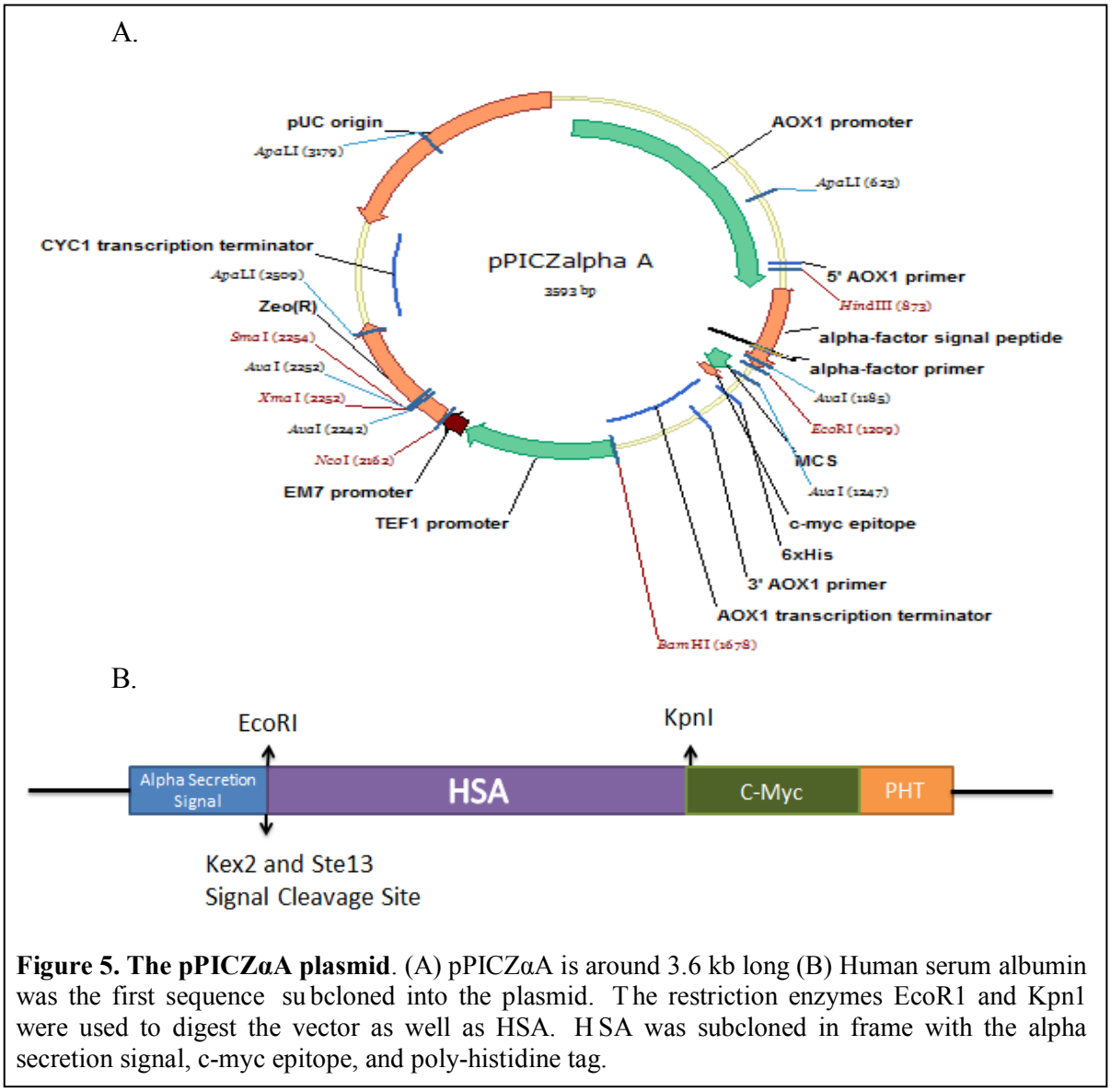

Figure 5. The pPICZαA plasmid. (A) pPICZαA is around 3.6 kb long (B) Human serum albumin was the first sequence subcloned into the plasmid. The restriction enzymes EcoR1 and Kpn1 were used to digest the vector as well as HSA. HSA was subcloned in frame with the alpha secretion signal, c-myc epitope, and poly-histidine tag.

terminal side of HSA (Fig. 7A). These inserts also contained a (6X) glycine polylinker, and these plasmids were named pPICZαA hEP-HSA, and pPICZαA mEP-HSA. All the constructs which contained mEP served to produce recombinant protein as a negative control, since mEP alone was shown to be less potent in blocking HCV entry into Huh7.5.1 cells. Once diagnostic

double digestions were performed using EcoR1 and Kpn1, and two bands of the appropriate sizes were present (3.6 kb and 2.0 kb), the plasmids were then sent for Sanger sequencing (Fig 6B, Fig 7B). All fragments were successfully subcloned into pPIZαA.

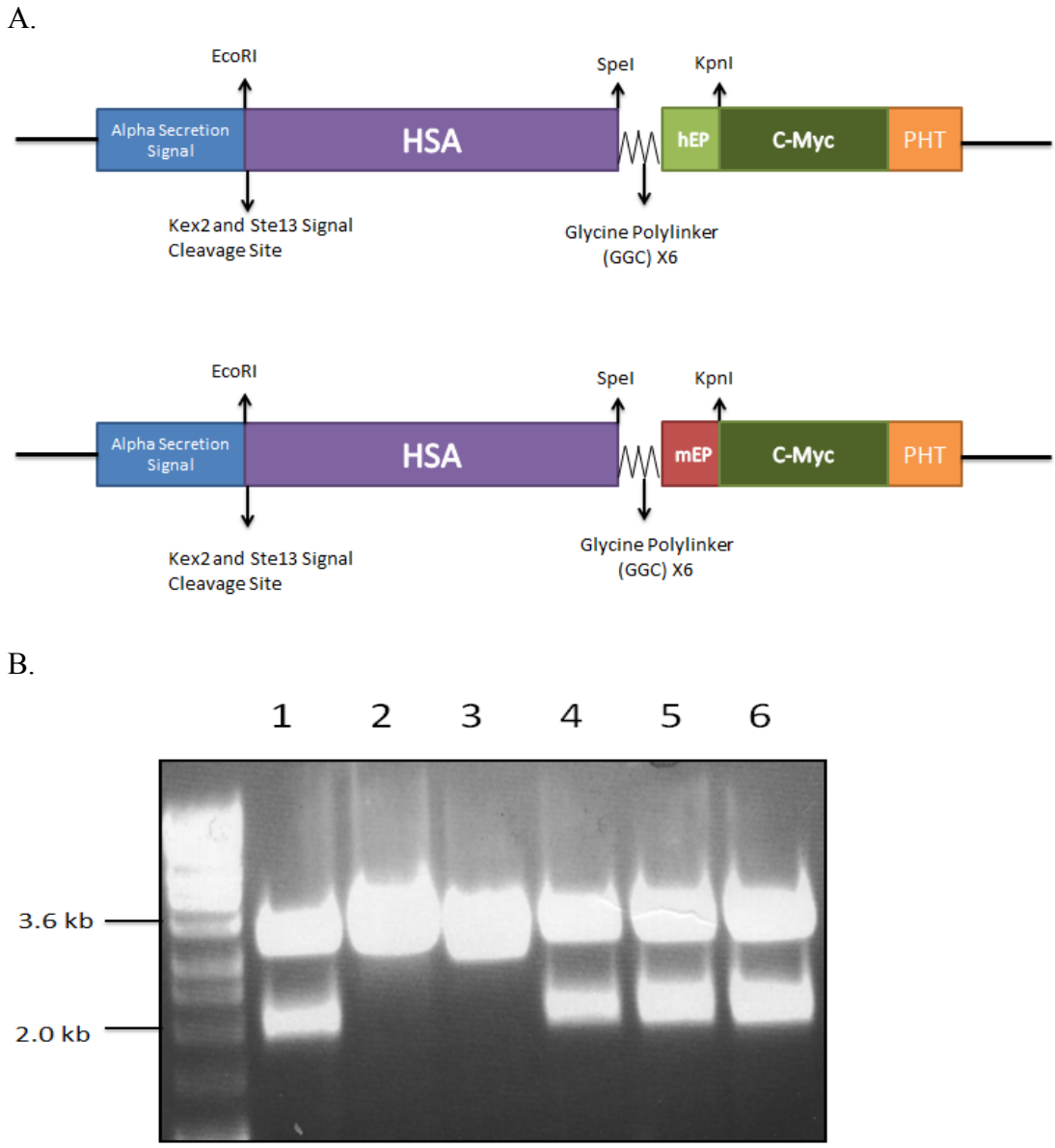

Figure 6. Subcloning of hEP and mEP C terminally to HSA. (A) Subcloning scheme for pPICZαA HSA-hEP and pPICZαA HSA-mEP (B) Diagnostic digestion of pPICZαA HSA-hEP and pPICZαA HSA-mEP. Lane 1 represents successful double digestion of pPICZαA HSA-hEP, and lanes 4, 5, and 6 represent successful digestions of pPICZαA-HSA-mEP. The DNA for both constructs was double digested with EcoR1 and Kpn1.

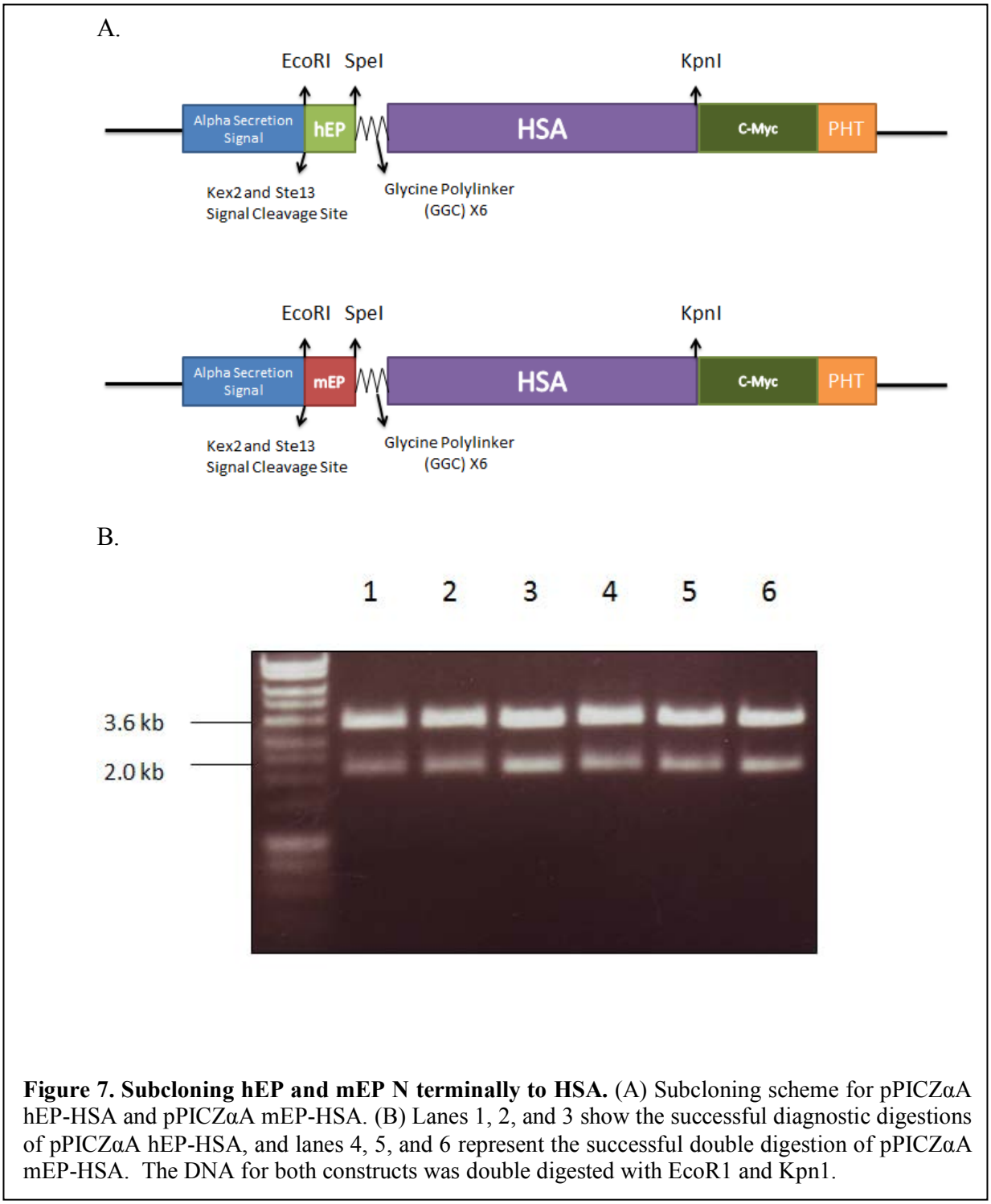

Figure 7. Subcloning hEP and mEP N terminally to HSA. (A) Subcloning scheme for pPICZαA hEP-HSA and pPICZαA mEP-HSA. (B) Lanes 1, 2, and 3 show the successful diagnostic digestions of pPICZαA hEP-HSA, and lanes 4, 5, and 6 represent the successful double digestion of pPICZαA mEP-HSA. The DNA for both constructs was double digested with EcoR1 and Kpn1.

4.1.2 Electroporation of X-33 *Pichia Pastoris*

Once the Sanger sequencing results showed that our plasmids contained the proper inserts, 10 µg of each plasmid were linearized using the PmeI restriction enzyme in order to be

electroporated into electrocompetant X-33 *Pichia pastoris*. During electroporation, the linearized plasmids entered the nucleus of the yeast cell and were incorporated into the host 5' AOX1 site (Fig. 8). After the electroporation, different volumes of cells (25 µL, 50 µL, 100 µL, 200 µL) were spread on 100 µg/mL zeocin YPDS plates (Fig. 9A). The plates were

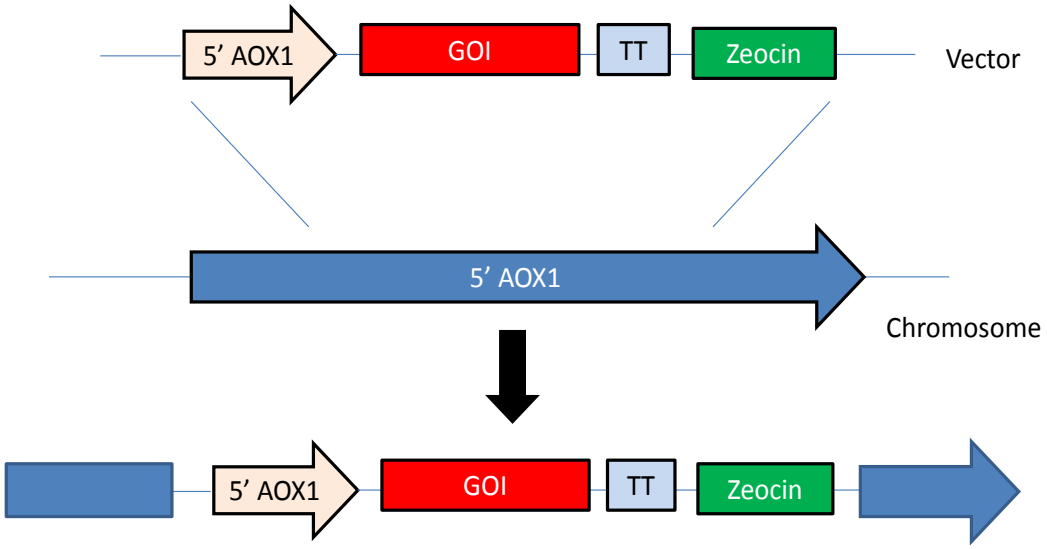

Figure 8. Plasmid integration. During electroporation, the linearized plasmids were incorporated into the host chromosome at the 5' AOX1 region. The pink arrow represents the AOX1 promoter region in the plasmid, GOI represents the gene of interest, TT is the transcription termination region, and the green box represents the zeocin resistance gene.

incubated at 30º C for three days, and 12 colonies from each electroporated construct were picked and streaked on 100 µg/mL zeocin YPDS plates. This was done to ensure that the colonies contained the integrated construct. If the colony was a false positive, than it should not have grown on a zeocin YPDS plate after it was streaked. Only one false positive was identified when streaking an HSA-hEP colony. The false positive failed to grow on a 100 µg/mL zeocin YPDS plate. The negative control in the experiment was taking X-33 *Pichia pastoris* that had been electroporated without any linearized plasmid DNA and spreading the cells on 100 µg/mL

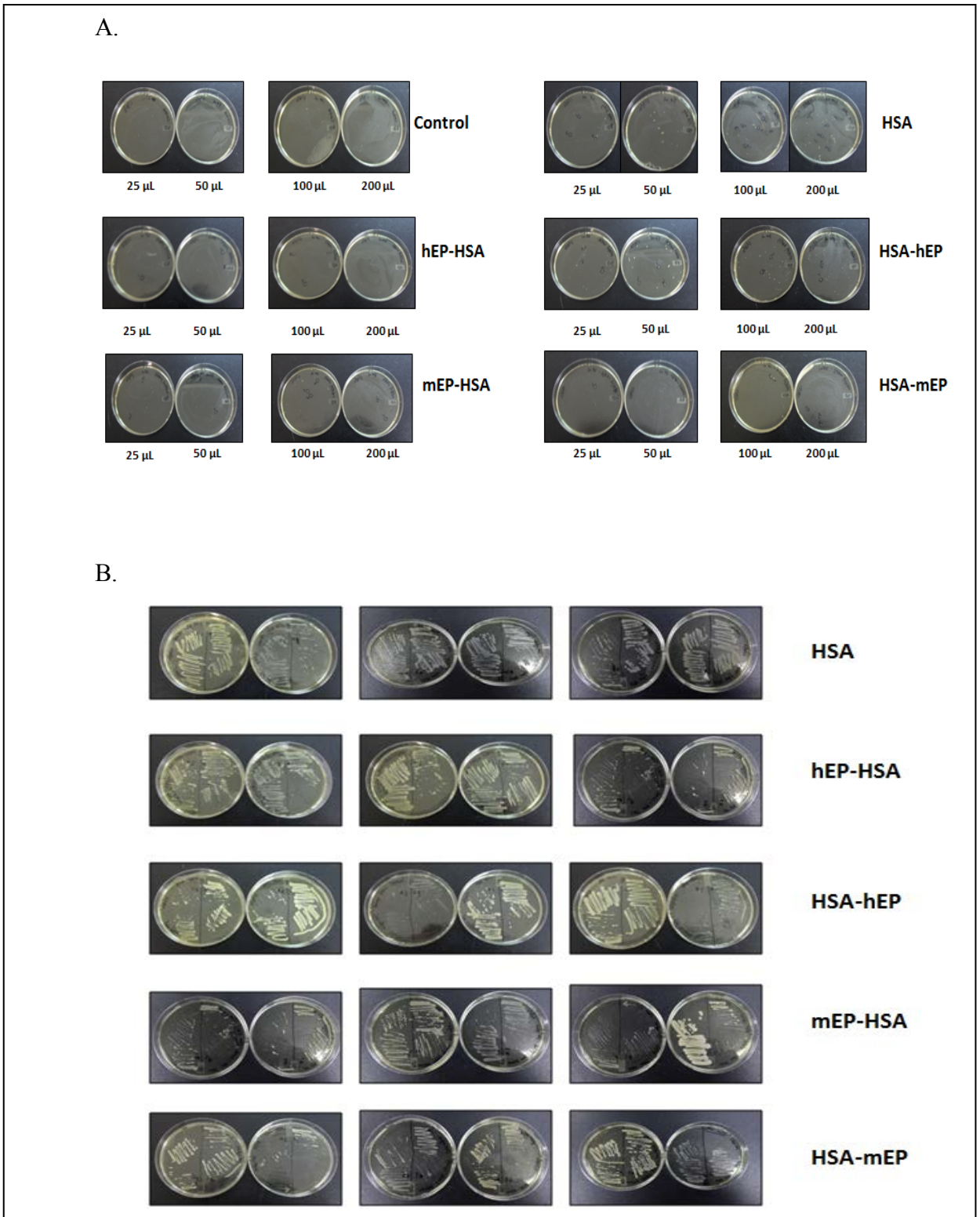

Figure 9. Plating and purifying of electroporated X-33 *Pichia pastoris*. (A) After electroporation, the listed volumes of cells were spread on 100 µg/mL zeocin YPDS plates. For all four plates, each construct had these many total colonies: control – 0 colonies, HSA – 58 colonies, hEP-HSA – 14, HSA-hEP – 89, mEP-HSA – 49, HSA-mEP – 17 (B) Twelve colonies were picked and purified on 100 µg/mL zeocin YPDS plates, and then 500 µg/mL zeocin YPDS plates which is shown above. We looked to see which colonies grew robustly on the 500 µg/mL zeocin YPDS plates.

zeocin YPDS plates. There were no colonies on any of the control plates. To further purify the colonies and ensure they contained the integrated plasmid, they were streaked on 500 µg/mL zeocin YPDS plates (Fig. 9B). All robust colonies were further analyzed for the presence of the inserted plasmid.

4.1.3 Colony PCR of Electroporated of X-33 *Pichia pastoris*

In order to prove that the linearized plasmid DNA was incorporated into the host genome, a colony PCR procedure was performed using primers designed specifically for the AOX1 regions in the plasmid, as well as primers specific for one of the inserts. pPICZαA was designed with an AOX1 forward and reverse region where primers could be used to detect the presence of the gene of interest. When performing a colony PCR on electroporated X-33 *Pichia pastoris* using the AOX1 forward and reverse primers, two bands should be present once the process is finished. The first band should be 2.2 kb long, and this represents a natural endogenous region. The second band should correspond to the gene of interest. In our case, for all the constructs containing mEP or hEP, the band sizes we expected to see were 2.6 kb. We never saw any bands this size. Next, we tried different combinations of primers. For the constructs where hEP and mEP were N terminal to HSA, the AOX1 forward primer was used along with either the hEP or mEP reverse primers. These bands were 536 base pairs long and were detected for some of the colonies (Fig. 10B and D). For the constructs where hEP and mEP were C terminal to HSA, the AOX1 reverse primer was used along with the hEP or mEP forward primers. These bands were 381 base pairs long, and were also detected in some of the colonies (Fig. 10A and C). The colonies containing HSA were detected using AOX1 forward and HSA reverse primer (Fig.

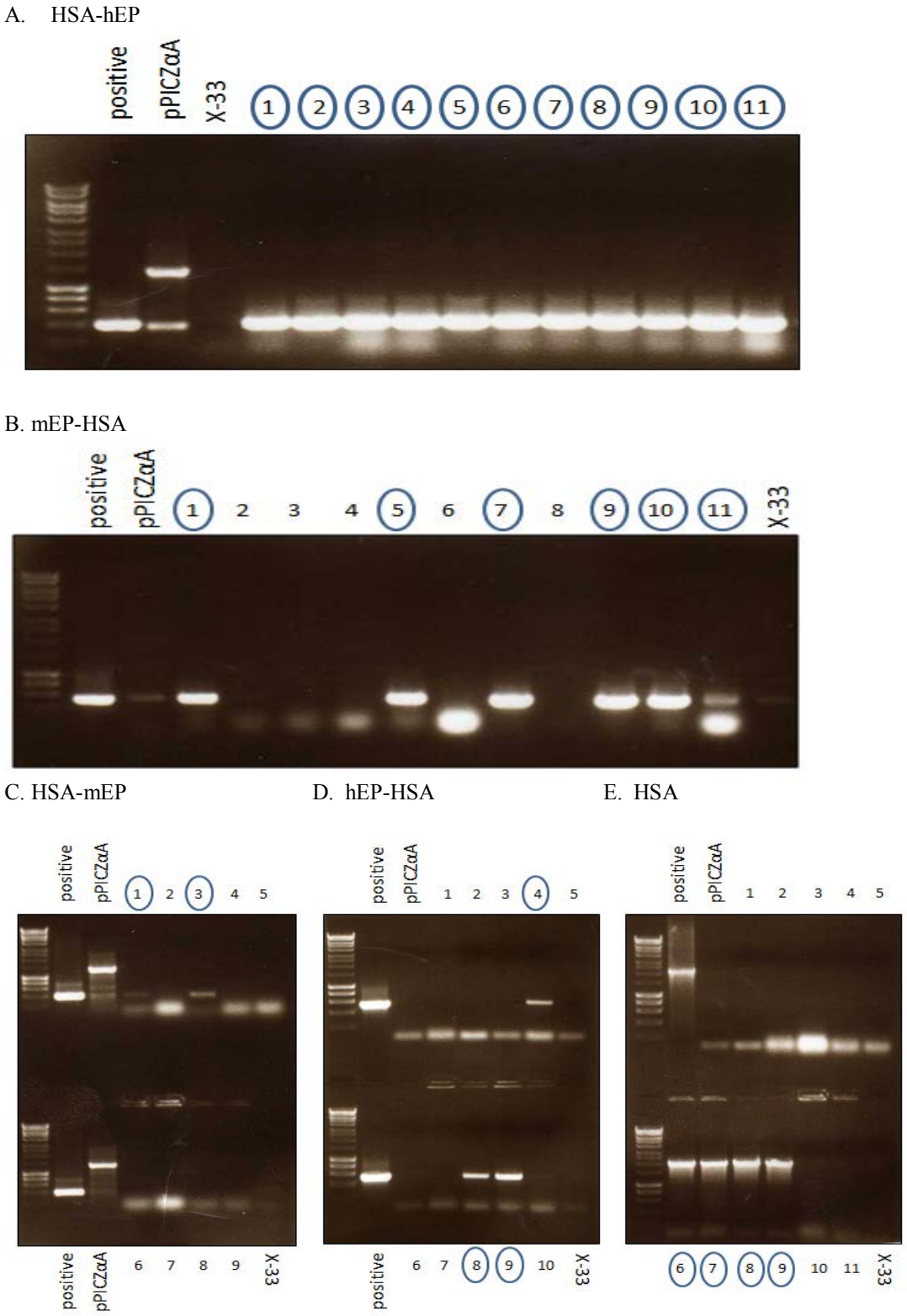

Figure 10. Electorporated X-33 colony PCR. All positive controls were the parent plasmids alone. The negative controls were pPICZαA and X-33 *Pichia pastoris*. (A) All HSA-hEP colonies analyzed were positive for a 381 base pair fragment. (B) Six lanes for mEP-HSA colonies were positive for a 536 base pair fragment: Lanes 1, 4, 7, 9, 10, 11. (C) Two lanes for HSA-mEP colonies were positive for a 381 base pair fragment: Lanes 1 and 3. (D) Three lanes for hEP-HSA colonies were positive for a 536 base pair fragment: Lanes 4, 8, and 9. (E) Four lanes for HSA colonies were positive for a 2,184 base pair fragment: Lanes 6, 7, 8, and 9.

10E), and were 2,184 base pairs long. For all our electroporated yeast clones, there were positive identifications of the integrated plasmids through colony PCR. The combination of robust colony growth on increasing concentraions of zeocin YPDS plates, as well as successful colony PCRs gave us confirmations that the electroporated X-33 *Pichia pastoris* contained the sequences needed for recombinant protein production.

4.2 SPECIFIC AIM 2 RESULTS

Aim 2: Produce the recombinant proteins of interest, and test the anti-HCV effects in cell culture using Huh7.5.1 cells and HCVcc luciferase

4.2.1 Recombinant Protein Production

After it was proven through colony PCR which electroporated yeast colonies contained the genes of interest, they were then used for recombinant protein production. For each construct, a single colony was picked and used to inoculate 25 mL of BMGY media. Once the OD_{600} reached 2, the culture was spun down, and the pellet was resuspended in 200 mL of BMMY. The presence of methanol as the sole carbon source was responsible for recombinant protein production, as it induced transcription from the AOX1 promoter. As shown in (Fig. 11), we first wanted to see if there was an optimal time for yeast growth. In order to determine when yeast growth was best, we took OD_{600} readings every twelve hours post BMMY inoculation for a total of 108 hours. We analyzed the growth of yeast colonies containing hEP-HSA, mEP-HSA, and standard X-33 *Pichia pastoris*. The 48 hour time point was shown to be optimal not only for

yeast growth, but for protein production as well. While taking yeast time point samples every 24 hours for five days and analyzing a clone containing HSA, the 48 hour time point showed

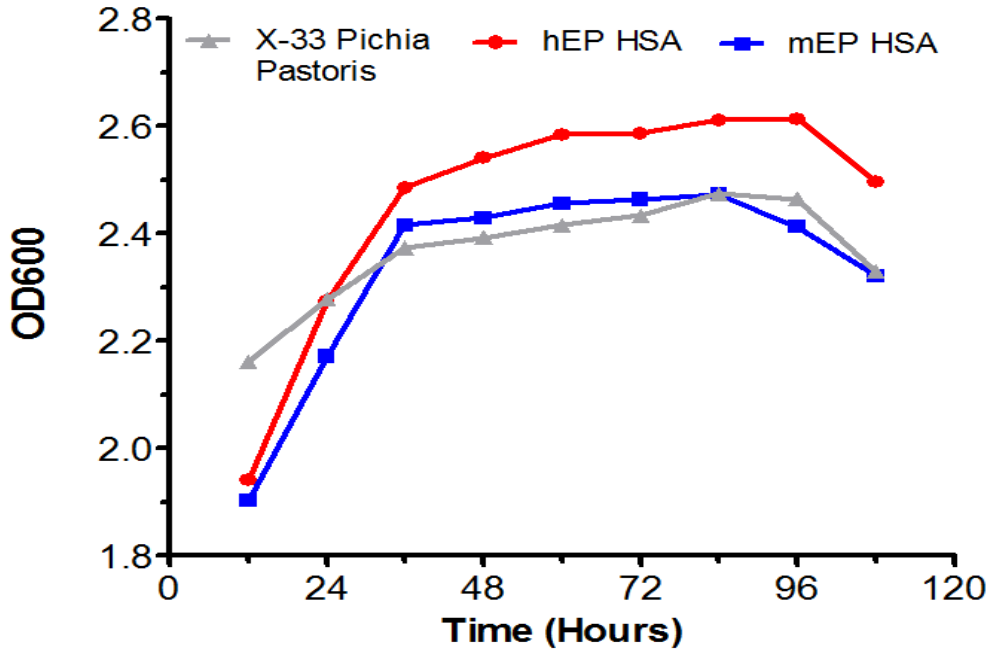

Figure 11. OD_{600} readings. OD_{600} readings were taken every 12 hours for the yeast cultures with clones hEP -HSA, mEP-HSA, and X-33 *Pichia pastoris*. OD_{600} of 1 = 5 x 10^7 cells.

the most prominent protein band when analyzing the lysates via Western blot (Fig. 12A). Therefore, after 48 hours of culture growth for a ll clones, they were spun down and the supernatants and pellets were both analyzed for the presence of recombinant protein. The cell lysates contained all the proteins of interest when analyzed by Western blot (Fig. 12B). We expected the HSA band to be around 73 kDa, and the bands which contain hEP and mEP to be around 79 kD a. HSA showed the strongest band, and doublets were observed for all the constructs. We believe that this is because the larger band may still have contained the alpha secretion factor, whereas the lower bands had it cleaved. For the proteins that contained the alpha secreation factor, they were 10 kDa longer than the proteins without it.

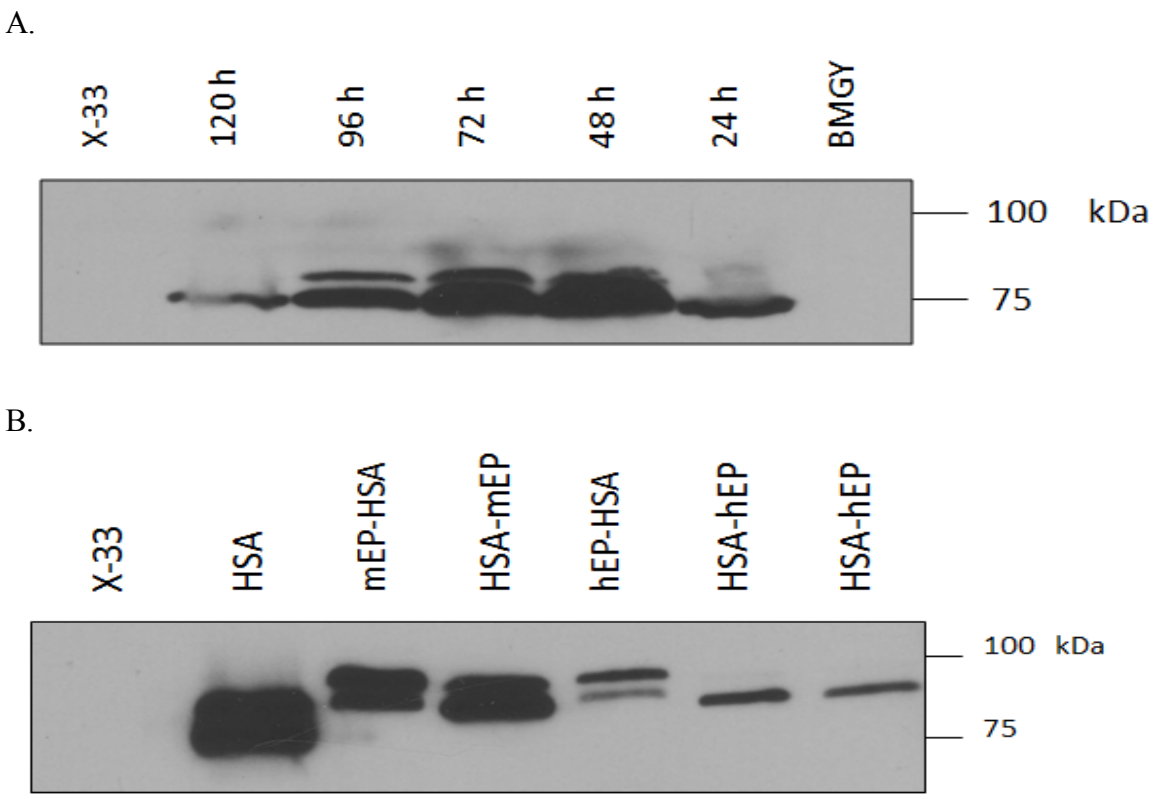

Figure 12. Recombinant protein production. (A) 1 mL time points from an HSA culture were taken every 24 hours for 5 days, and the cell pellets were analyzed for recombinant protein production via Western blot using a rabbit polycolonal anti-histidine antibody. A BMGY pellet along with an X-33 *Pichia pastoris* pellet served as negative controls. (B) Cell pellets from 200 mL BMMY cultures for all the clones were collected after 48 hours and analyzed for the presence of recombinant protein using a rabbit polyclonal anti-histidine antibody. A standard X-33 *Pichia pastoris* pellet served as a negative control.

4.2.2 Recombinant Protein Purification

The process of trying to purify our recombinant proteins of interest proved difficult. We used Ni-NTA agarose beads because the Ni resin is able to bind to the 6X histidine tag on the recombinant protein. Since we were only able to isolate secreted recombinant protein at very low concentrations, we attempted to isolate our proteins from the yeast cell lysates. The only recombinant protein we were able to purify from the lysates using Ni-NTA agarose beads was HSA. We were not able to successfully isolate any of the others. We analyzed the cell debris from the hEP an mEP pellets via Western blot after lysis and centrifugation, and the protein

bands observed were very thick (data not shown). If we spun the lysate at 12,000 rpm for ten minutes and then tried to detect protein in the supernatant, there was very little to nothing at all that could be detected via Western blot. Our Coomassie blue staining and Western blot of HSA showed that we were able to purify it using 200 mM imidazole (Fig. 13). Further evidence of our isolation was shown by mass spectrometry, which was performed on the cut out 200 mM imidazole Coomassie blue stained lane by one of our lab's coworkers, Ting Zhao. The results were not only positive for the presence of HSA, but showed HSA was the most abundant protein (Fig. 14B and C). In order to try and remove any insoluble protein from the cell debris from the hEP and mEP pellets, we treated the cell debris pellets with 1% Triton X-100. This however did not recover the insoluble recombinant protein. With these results, we thought it would be best

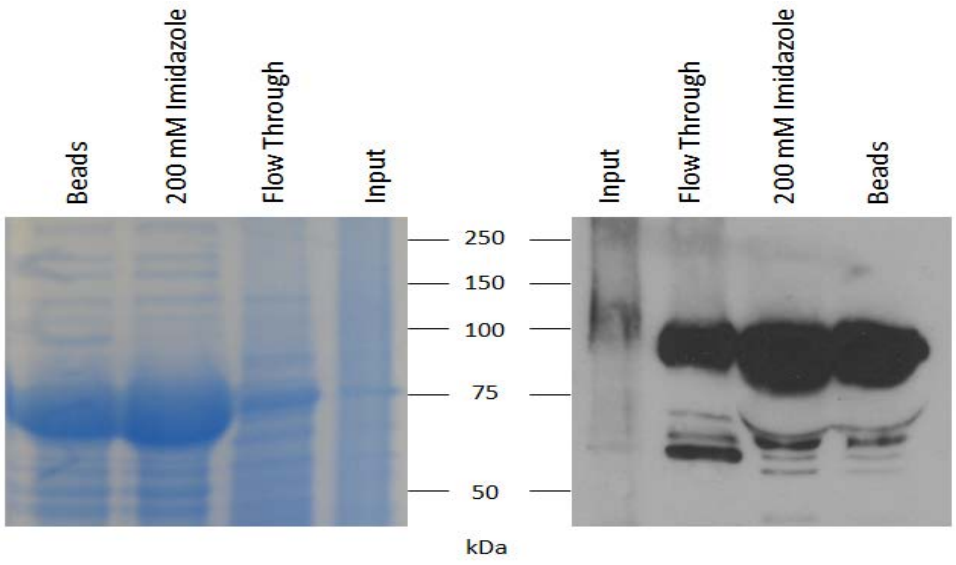

Figure 13. Purification of HSA. Prior to the batch purification, part of the input lysate was kept to be analyzed. After the Ni-NTA beads rotated with the lysate, the tube was spun down, and part of the flow through was also kept for analysis. The beads were then treated with 200 mM imidazole which was collected, and then the beads were added to 2X sample buffer and boiled to see if there was any leftover bound recombinant protein.

to test the whole cell lysate in cell culture to see whether or not there was any bioactivity among the recombinant proteins.

A.

- MKWVTFISLLFLFSSAYSRGVFRRDAHKSEVAHRFKDLGEENFKALVLIAFAQYLQQCPF
- EDHVKLVNEVTEFAKTCVADESAENCDKSLHTLFGDKLCTVATLRETYGEMADCCAKQEP
- ERNECFLQHKDDNPNLPRLVRPEVDVMCTAFHDNEETFLKKYLYEIARRHPYFYAPELLF
- FAKRYKAAFTECCQAADKAACLLPKLDELRDEGKASSAKQRLKCASLQKFGERAFKAWAV
- ARLSQRFPKAEFAEVSKLVTDLTKVHTECCHGDLLECADDRADLAKYICENQDSISSKLK
- ECCEKPLLEKSHCIAEVENDEMPADLPSLAADFVESKDVCKNYAEAKDVFLGMFLYEYAR
- RHPDYSVVLLLRLAKTYETTLEKCCAAADPHECYAKVFDEFKPLVEEPQNLIKQNCELFE
- QLGEYKFQNALLVRYTKKVPQVSTPTLVEVSRNLGKVGSKCCKHPEAKRMPCAEDYLSVV
- LNQLCVLHEKTPVSDRVTKCCTESLVNRRPCFSALEVDETYVPKEFNAETFTFHADICTL
- SEKERQIKKQTALVELVKHKPKATKEQLKAVMDDFAAFVEKCCKADDKETCFAEEGKKLV
- AASQAALGL

B.

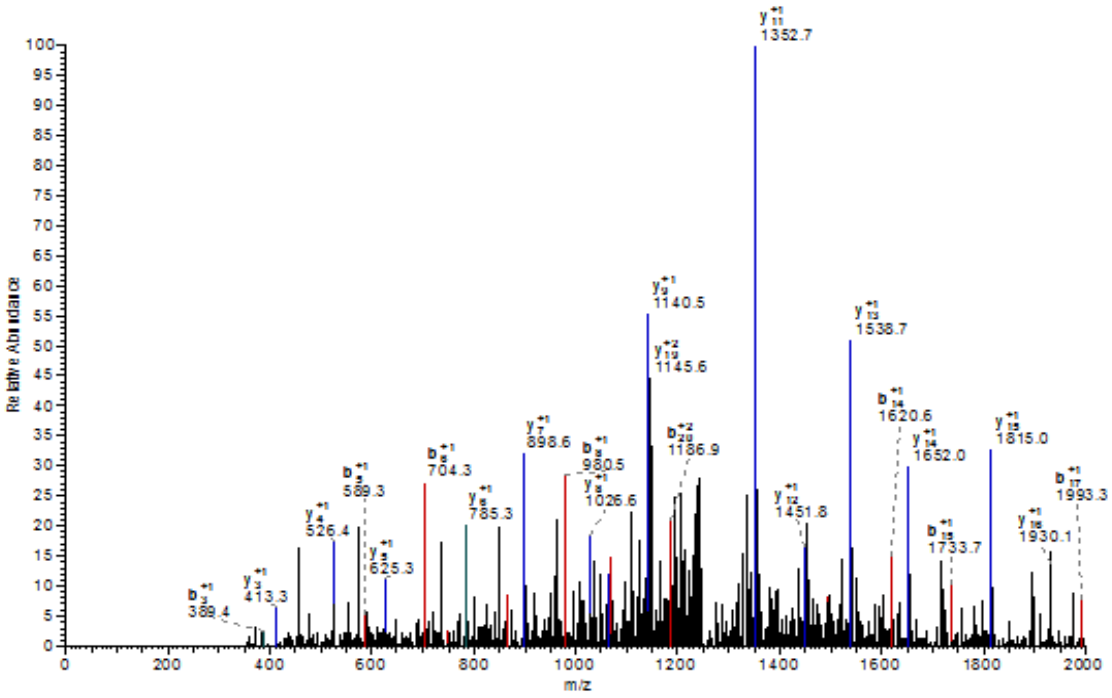

C.

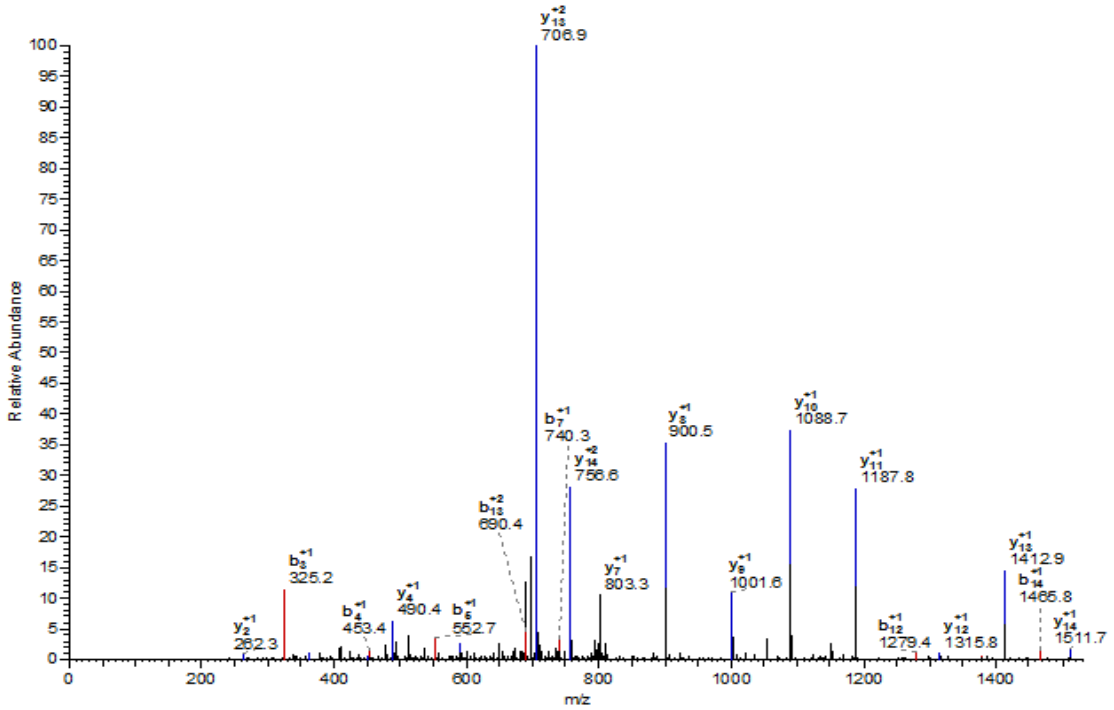

Figure 14. Mass spectrometry results from Coomassie blue staining containing HSA. Above are two representative regions of HSA identified through mass spectrometry of the cut out 200 mM imidazole Coomassie blue stained lane. (A) The coverage sequence used in identifying HSA, with the regions in red representing analyzed portions. (B) Identified region in HSA with the amino acid sequence MPC#AEDYLSVVLNQLCV#LHEK. The m/z was 1352.7 (C) Identified region in HSA with the amino acid sequence KVPQVSTPTLVEVSR. The m/z was 706.9.

4.2.3 Quantification of Protein

Before testing the cell lysate in cell culture, it was necessary to quantify the total protein in each lysate, as well as the individual recombinant proteins. A BCA assay kit was used in order to quantify the total protein in each lysate. The first step in quantifying the protein was to create a standard curve using a known amount of protein. This protein was provided in the kit, and the standard curve created gave us a linear line of best fit. From there, we were then able to quantify the total protein amount in each lysate using the UV spectrophotometer (Table 6). After quantifying the total amount of protein in each lysate, we next set out to determine the total amount of recombinant protein. In order to do this, we created a standard using a His-tag protein

with a known concentration. The protein we chose for this was Tat Cre which was produced in our lab. We started by loading different amounts (1 µg, 500 ng, 400 ng, 300 ng, 200 ng, 100 ng) of Tat Cre on an 8% SDS gel, and then loaded 8 µL of each of our lysates. Based on the results of the Western blot, we were able to determine the amount of recombinant protein in each lysate by comparing the band intensity to the Tat Cre protein standard. The amount of recombinant protein was low for all the proteins except HSA. For HSA-hEP, hEP-HSA, and mEP-HSA, we determined the concentration was 12.5 µg/mL (Fig. 15A and B). HSA-mEP had a concentration of 37.5 µg/mL (Fig. 15B), and HSA had a concentration of 125.0 µg/mL.

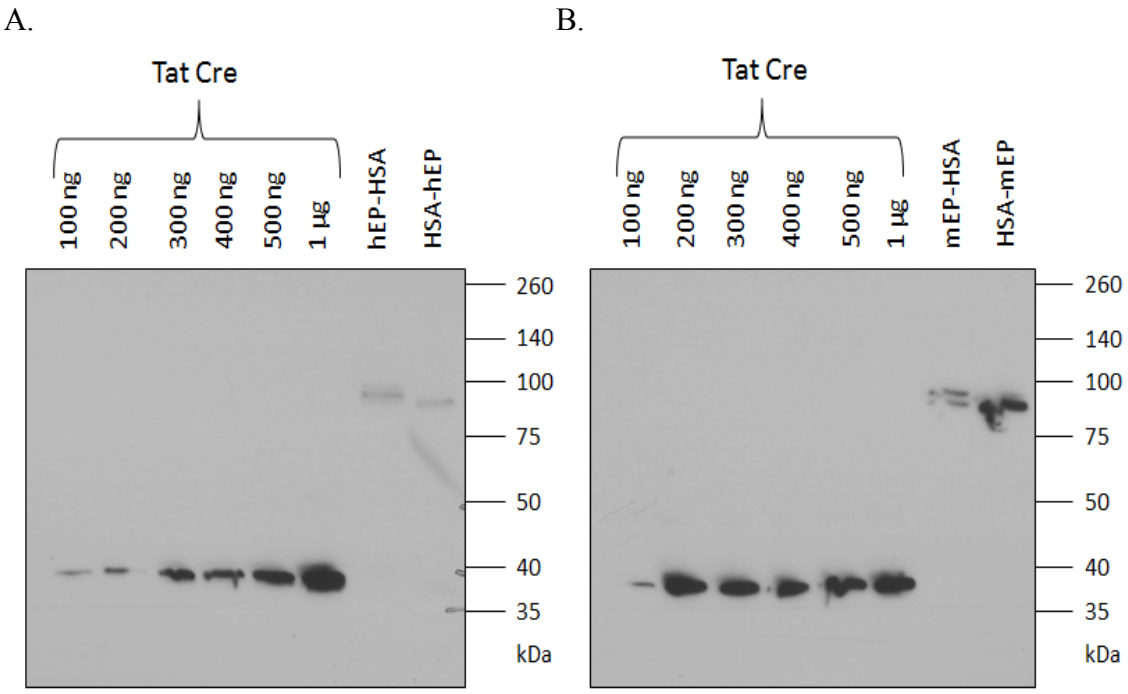

Figure 15. Recombinant protein concentration. (A) 8 µL of hEP-HSA and HSA-hEP lysate were loaded onto an 8% SDS gel and run along a (6X) His -tagged Tat Cre protein standard. Both proteins had a concentration of 12.5 µg/mL (B) 8 µL of mEP-HSA and HSA-mEP were loaded under the same conditions. The concentration of mEP-HSA was 12.5 µg/mL, and HSA-mEP was 37.5 µg/mL The exposure time on the films shown above was 1 second. 5 second and 30 second exposures were also done, and there was linearity in band intensity among the increased exposure times.

Table 6. Concentration of total protein in cell lysates

Lysate Protein	Concentration
X-33 *Pichia pastoris*	9,787 µg/mL
HSA	12,830 µg/mL
HSA-hEP	13,960 µg/mL
HSA-mEP	13,250 µg/mL
mEP-HSA	17,250 µg/mL
hEP-HSA	24,020 µg/mL

4.2.4 Concentration of Protein

In order to increase the concentration of our recombinant proteins, we decided to concentrate our lysates by using a centrifugal device that would retain all proteins greater than 30 kDa. We took 5 mL of each of our lysates and concentrated them to 500 µL, after which, we then added the concentrated lysate to 10 mL of PBS to dilute the salts in the breaking buffer. We then concentrated the diluted lysate back to 500 µL. This increased the concentration of our recombinant proteins. Western blot analysis of the concentrated lysates indeed showed that the concentration worked, as the intensity of the bands had increased (Fig. 16). The total protein concentration was shown to have increased (Table 7). We estimated that the concentration of HSA increased to 250 µg/mL, and the concentrations of hEP-HSA, mEP-HSA, and HSA-mEP increased to 100 µg/mL (Fig. 16A and B). HSA-hEP had the lowest concentration of 62.5 µg/mL (Fig. 17A).

Table 7. Concentration of total protein in concentrated lysates

Total Protein	Concentration
X-33 *Pichia pastoris*	21,800 µg/mL
HSA	39,770 µg/mL
HSA-hEP	32,410 µg/mL
HSA-mEP	25,770 µg/mL
mEP-HSA	33,540 µg/mL
hEP-HSA	37,580 µg/mL

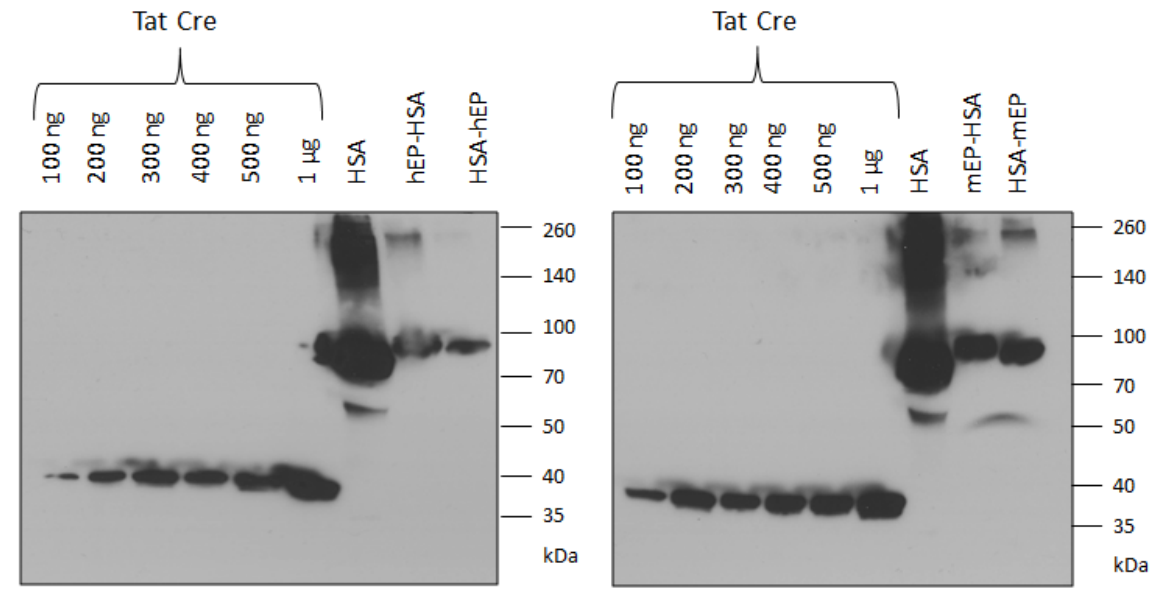

Figure 16. Concentration of recombinant protein after centrifugal concentration. (A) Here shown is concentrated HSA, hEP-HSA, and HSA-hEP. It was determined that that the HSA concentration was 250 µg/mL, hEP-HSA was 100 µg/mL, and HSA-hEP was 62.5 µg/mL. (B) The concentrations of mEP-HSA and HSA-mEP was determined to be 100 µg/mL. The exposure time on the film was 1 second.

4.2.5 Infectivity Assay

We first analyzed the effects of HSA-hEP and HSA-mEP for the ability to inhibit HCVcc-luciferase infection. We tested 5 µg of both recombinant proteins in the concentrated lysates by adding them to the cells with the virus at the same time. 5 µg HSA was also tested. After a 3 hour incubation, the lysates and the virus were removed and replaced with fresh DMEM. When the luciferase reading was taken 48 hours later, we saw that there was a significant difference between all the recombinant proteins in inhibiting HCVcc luciferase infection compared to the infected/untreated wells (Fig. 17). We next wanted to see if hEP-HSA and mEP-HSA had an effect on inhibiting viral infectivity. 5 µg of each recombinant protein was tested, however there was no significant difference between the infected/untreated cells and the cells treated with lysates containing the recombinant proteins (Fig. 18). After determining

that not all of the recombinant proteins inhibited viral infection to a significant degree, we then wanted to compare the inhibitory effects of the recombinant proteins containing hEP or mEP

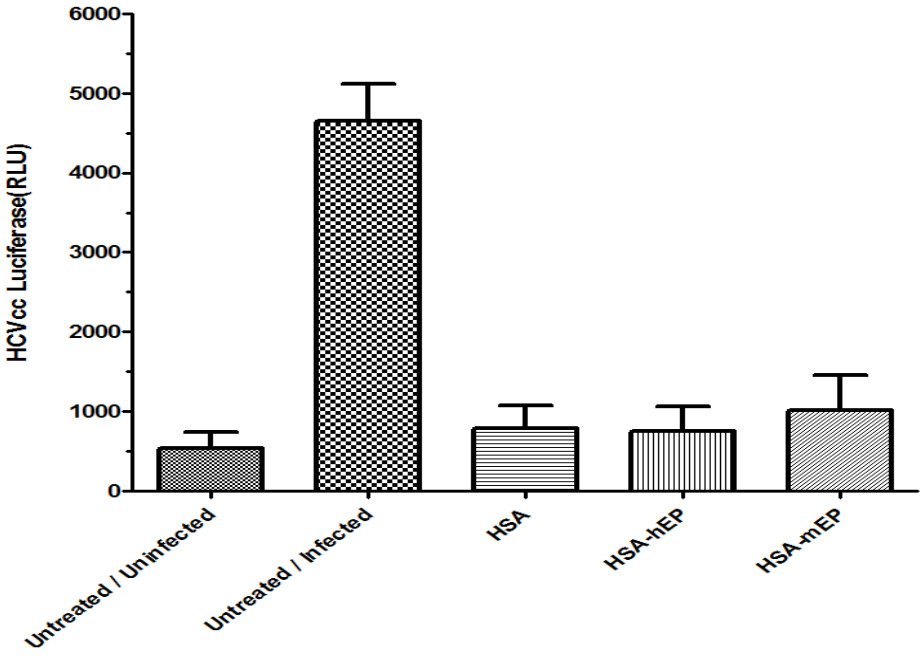

Figure 17. Effects of HSA-hEP and HSA-mEP. In order to test 5 µg of each recombinant protein, 20 µL of concentrated HSA lysate, 80 µL of HSA-hEP concentrated lysate, and 50 µL of HSA-mEP concentrated lysate were added in duplicate to wells containing Huh7.5.1 cells at 80% confluency. The total amount of protein in each volume of lysate added was 795.4 µg in the HSA lysate, 2,592.8 µg in the HSA-hEP lysate, and 1,289 µg in the HSA-mEP lysate. There was a significant difference between the untreated/infected cells and the cells treated with each of the lysates, as $p<0.05$ in all comparisons. Data are representative of three independent experiments and are presented as the mean ± standard deviation.

to that of HSA. The percent infection was calculated by dividing the relative light unit (RLU) value collected for cells treated with the mEP or hEP recombinant proteins by the RLU value for the cells treated with the HSA recombinant protein. The results showed that the cells treated with hEP-HSA had the lowest percentage of infection with an average of 57% cells infected compared to HSA (Fig. 19). The cells treated with HSA-mEP had a greater infection average than HSA. hEP-HSA looked to be the most promising recombinant protein in blocking HCVcc luciferase infection based on these results.

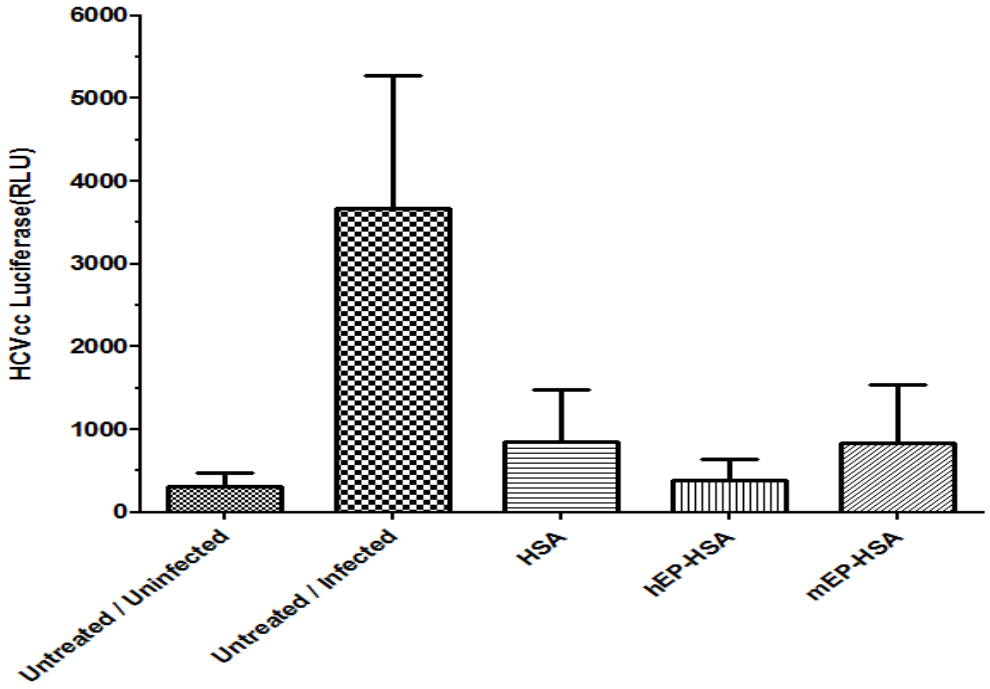

Figure 18. Effects of hEP-HSA and mEP-HSA. In order to test 5 µg of each recombinant protein, 20 µL of concentrated HSA lysate, and 50 µL of concentrated hEP-HSA and mEP-HSA lysates were added in duplicate to wells containing Huh7.5.1 cells at 80% confluency. The total protein amount in each volume of lysate added was 795.4 µg in the HSA lysate, 1,897 µg in the hEP-HSA lysate, and 1,677 µg in the mEP HSA lysate. There was no significant difference between the untreated/infected cells and the cells treated with the lysates, as $p>0.05$ in all comparisons. The data is representative of three independent experiments and are presented as the mean ± standard deviation.

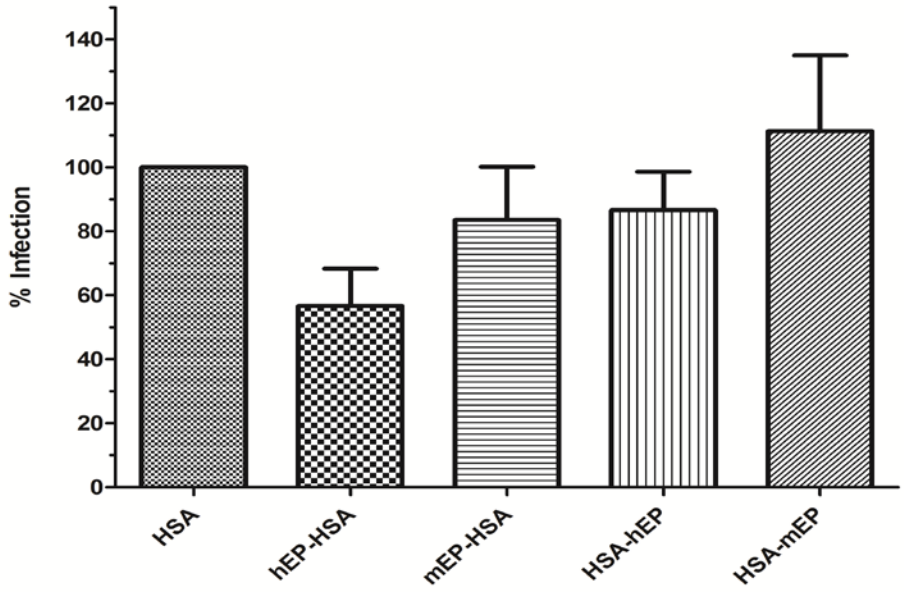

Figure 19. Percent infection. The average percentage of infected cells treated with the lysates containing hEP and mEP recombinant proteins were compared to cells treated with HSA lysate as follows: 57% for hEP-HSA, 84% for mEP-HSA, 87% for HSA-hEP, and 111% for HSA-mEP.

4.2.6 Cell Viability Assay

In order to determine if the cell lysate added to the Huh7.5.1 caused any cytotoxicity, cells were added to a 48 well plate and grown to 80% confluency. A cell viability assay was then performed. The cells in the wells were lysed, and the lysates was mixed with CPE buffer. Cellular ATP drove the oxidation of luciferan resulting in light emission which could be quantitated. We performed the cell viability assay using standard X-33 *Pichia pastoris* lysate. Different amounts of lysate were incubated with the cells for three hours, after which it was removed and replaced with fresh media. The cells were then lysed 48 hours later and a luciferase reading was taken to determine cell viability (Fig 20). Based on the results, we concluded that there was cytoxictiy involved when adding *Pichia pastoris* lysate to Huh7.5.1 cells.

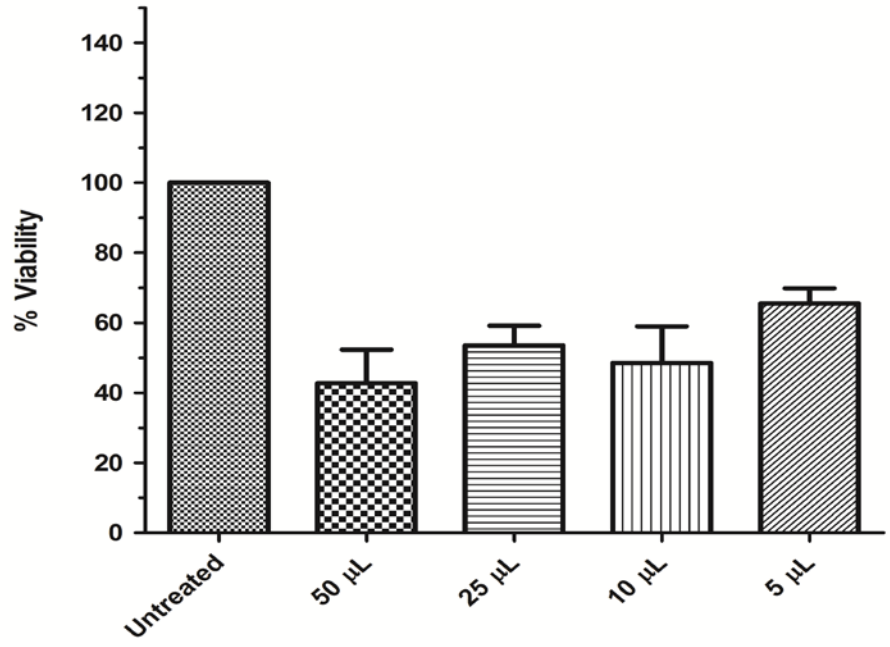

Figure 20. Cell viability. Different volumes of X-33 *Pichia pastoris* lysate were added to Huh7.5.1 cells in duplicate. The total protein added in each volume was 1,090 µg in 50 µL, 545 µg in 25 µL, 218 µg in 10 µL, and 109 µg in 5 µL. There was a significant difference, $p<0.05$, between the untreated cells and the cells treated with the different volumes tested. The data is representative of four independent experiments.

4.2.7 Confocal Microscopy

In order to visually examine the effects the lysates containing the recombinant proteins were having on viral infectivity, we treated Huh7.5.1 cells with lysates containing 2 µg of the hEP and mEP recombinant proteins as well as with JFH1-AM2 HCV. After a three hour incubation, the virus and lysates were removed and 48 hours later the cells were fixed for confocal imaging. Using primary antibodies against HCV core protein and E2 glycoprotein, and alexa-fluor conjugated secondary antibodies, we were able to visualize infection of the cells (Fig. 21). The positive control were cells treated with only the virus, and the negative controls were untreated/uninfected cells as well as cells treated with 2 µM hEP peptide and virus. There was a significant difference in percentage of infected cells between hEP-HSA and both mEP containing recombinant proteins. The hEP-HSA recombinant protein lysate showed the lowest average of percentage of cells infected (Fig. 22).

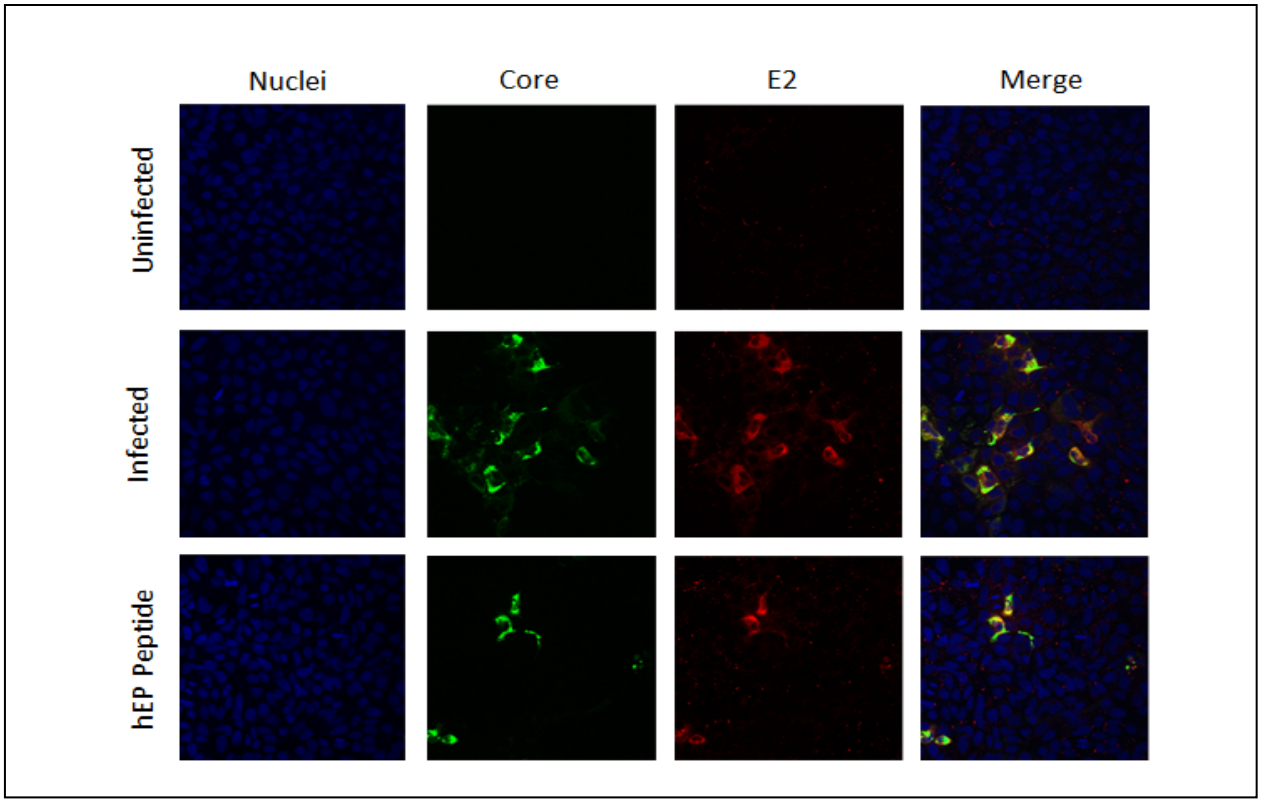

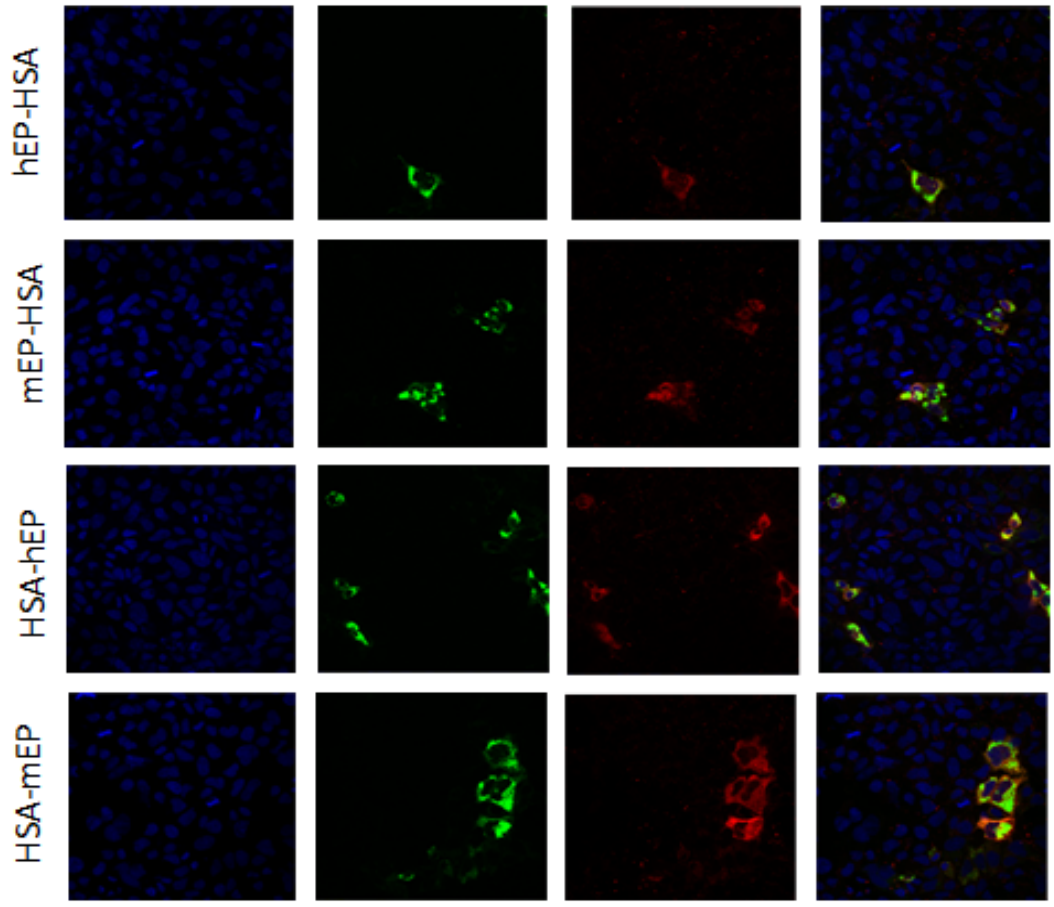

Figure 21. Immunostaining of Huh7.5.1 cells treated with concentrated lysate. The cells were grown between 80-90% confluency in a 24 well plate with coverslips. Each lysate was added to where the final recombinant protein amount was 2 µg. 2 µM of hEP peptide was tested as well. The images are representative of 3 random fields of view taken, and include Draq5 nuclei staining, core protein detection, E2 glycoprotein detection, and a merge between the three.

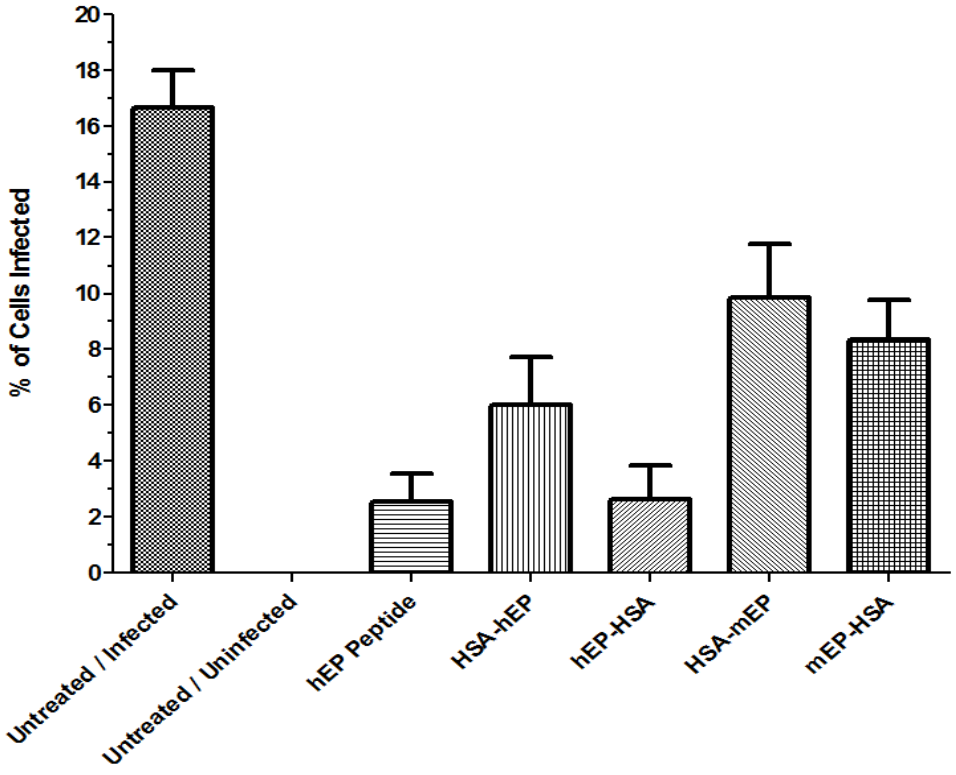

Figure 22. Percentage of infected cells. The percentage of infected cells was determined by taking the number of infected cells in each field of view (3 total), and dividing that number by the total amount of Draq5 stained nuclei. The percentages of calculated for each field of view was then averaged. There was a significant difference, ($p<0.05$), between the hEP-HSA average, and the averages between both mEP recombinant protein treated cells.

5.0 DISCUSSION

The ability to target HCV entry into human hepatocytes looks to be a promising way to develop novel anti-viral therapeutics. The accepted host factors which are involved in HCV entry are heparan sulfate, low-density lipoprotein receptor, CD81, SR-B1, claudin-1 and occludin. In addition to the aforementioned receptors, host derived apolipoprotein E is now recognized as a component of the infectious HCV particle. Apo E is needed for both infectivity and viral assembly, and is also able to aid the virus from immune evasion. Since apo E is a protein produced by the host, it does not elicit any kind of immune reaction. The amount of apo E present on the viral particle is also proportional to infectivity (21). The more apo E present, the more infectious the particle will be. Apo E molecules present on infectious HCV particles outnumber the amount of E2 glycoprotein, providing more evidence for its aid in infection (66). Based on the structure of apo E, our lab developed the novel peptide, hEP, to outcompete virion associated apo E for the binding of the necessary attachment receptors. We know that this peptide prevents entry at an early stage, because it prevented viral binding to cells either by blocking HSPG, LDLR, or a different unknown receptor. Just this year however, it was reported that HCV attachment to susceptible cells is mediated by virion associated apo E binding to HSPG (50). When the LDLR receptor was knocked down using siRNA, viral infectivity decreased by 80%, but HCV was still able to bind to Huh7.5 cells with high affinity. This group also performed an experiment where anti-apo E antibodies were added to the cells at the same

time as the virus, or after viral binding. When added after viral binding, there was no inhibition of viral entry. All together, these results give indirect evidence that the hEP peptide may indeed bind to HSPG in order to block infection. Unlike the current drugs boceprevir and telaprevir which target viral proteins, hEP targets the host cell, which is a major advantage because there is little possibility of the virus gaining resistance.

When trying to determine whether or not the effects of hEP could be amplified, we hypothesized that fusing it to HSA would create a fusion protein with increased pharmacokinetics. When another group fused HSA to IFN-α, they showed that this fusion protein named Albuferon required less dosing and was more potent on a molar basis than just standard IFN-α (78). The effects of HSA enabled Albuferon to have an 18-fold longer half-life than just standard IFN-α when tested in cynomolgus monkeys. We predicted that the same effects would occur with HSA fused to hEP. Using the methlylotropic X-33 *Pichia pastoris* yeast strain, we showed that we were able to produce our fusion proteins of interest. This particular system was designed to secrete out our proteins of interest, however we never successfully isolated secreted protein to a suitable concentration. Even when we used Ni-NTA beads to isolate secreted recombinant protein, we barely were able collect any. We tried many methods in troubleshooting to try and induce secreted protein expression, but were unsuccessful. We were only able to identify our proteins when we lysed the yeast cells. From the cell lysates, the only recombinant protein we successfully isolated was HSA. We believe that the lipid binding regions of the recombinant proteins which contained mEP or hEP made them insoluble, and difficult to isolate. Standard hEP was shown to be insoluble in water due to the presence of the lipid binding region derived from apo E (58).

A method that could be performed in the future to determine whether the recombinant proteins containing hEP or mEP are insoluble would be to do an immunostaining on electroporated X-33 *Pichia pastoris* cells which contain the genes of interest and had been grown in BMMY. This would allow us to visualize whether or not the recombinant proteins were insoluble and clumped together within the cells themselves. The methanol in the media will trigger recombinant protein production and using a primary antibody against the (6 X) histidine tag, as well as an alexa-fluor conjugated secondary antibody would allow us to visualize the location of the recombinant proteins intracellularly. Perhaps they may be clumped in the endoplasmic reticulum, or they may be trapped in between the cell membrane and the cell wall. This visual would give insight to where the insoluble recombinant protein may be sticking to in the cell debris.

After testing the lysates containing our recombinant proteins on Huh7.5.1 cells, we did see an inhibitory effect caused by 5 µg of hEP-HSA recombinant protein in cell culture as well as when immunostaining cells treated with 2 µg of hEP-HSA. Based on our results, we believe that hEP-HSA has more promise in being an effective inhibitor than HSA-hEP. The fact that hEP-HSA has the hEP region exposed at the N-terminal side of the protein may make it more effective, unlike HSA-hEP where the hEP portion was between HSA and the C-terminal tag. Being in between HSA and the tag may have potentially inhibited its function.

Even though we diluted the lysates in 1X PBS at a 1:20 ratio, there still was cytotoxicity. This all stemmed from the fact that we were never able to successfully isolate all of our recombinant proteins, and therefore we decided to test our yeast cell lysates for bioactivity. Even when using 1% Trition X-100 to try and remove the insoluble protein from the cell debris pellet, we still were not able to isolate our hEP and mEP recombinant proteins. The cytotoxicity

may have been caused by the debris from the lysates. A detergent like urea could be used to remove insoluble proteins from the lysate if we ever attempt to purify the recombinant protein from the lysate again. This detergent however denatures proteins, which means they would have to be renatured in order to determine their effectiveness in a cell culture model.

In the future, we believe that the fusion of hEP-2 to HSA may be a better alternative than standard hEP fused to HSA. This is because hEP-2 only contains the LDLR binding region, and not the lipid binding region from apo E. It has already been shown that hEP-2 is soluble in water (58). At the time when we developed this project, we did not know whether or not hEP-2 would be as potent an inhibitor like we do now. It was still being tested for the ability to inhibit viral infectivity. In addition to using hEP-2, another alternative may be to perform an antibody purification rather than using Ni-NTA agarose beads. Since we were able to prove that HSA was produced, doing an HSA purification using a column coated with anti-HSA antibodies may be a more effective way of recombinant protein isolation. The size of HSA is around 70 kDa unlike the 6X His tag which is only 6 amino acids long. Due to the large size of HSA, the ability to bind antibodies in a column would be much easier.

Another alternative to using the standard *Pichia pastoris* expression system, is to try a different yeast secretion system such as PichiaPink. This system has the advantage of being able to easily identify positive electroporated transformants as they will turn white in color. In a recent publication, the investigators used the PichiaPink system to produce recombinant human interleukin 28B (23). This was a soluble protein, and they were able to optimize recombinant secreted protein expression to 200 mg/L. Since the fusion of HSA to hEP-2 would result in soluble protein, we may be able to produce secreted recombinant protein to the same level.

If we are able to successfully produce and purify hEP-HSA in the future and demonstrate it can elicit the same anti-viral effects with a longer half-life, additionally we would want to test its ability to bind lipids and suppress inflammation as well. We could start by testing hEP-HSA in cell culture for the ability to bind DMPC vesicles. If it is shown that it can bind to the same degree as hEP, then we would progress to testing for the ability to lower plasma cholesterol levels in mice as well as inflammation. People who are infected with HCV experience both an altered lipid metabolism as well as chronic inflammation which are very painful. The chronic inflammation is caused by the immune system's increased production of cytokines and chemokines which leads to liver fibrosis (55). Other drugs which have been shown to lower cholesterol include ezetimibie, fluvastatin, and Lovastatin. Ezetimibie not only lowers cholesterol, it was also shown to suppress HCV infection by inhibiting viral uptake by the newly identified receptor: Niemann-Pick C1-like 1(NPC1L1) (88). This drug inhibited infection of all the major HCV genotypes. Lovastatin and fluvastatin were also shown to lower viremia in infected individuals as well as pro-inflammatory cytokines (67). If the fusion of hEP to HSA is able to increase the pharmacokinetics of hEP, this would be an ideal therapeutic as it could inhibit viral infection, bind plasma cholesterol lowering hepatic steatosis, as well as suppress inflammation. The necessary dosage would be lower than standard hEP as well, which could lead to better patient compliance.

The application after showing in cell culture and in mice that hEP-HSA is effective in inhibiting viral entry, lowering plasma cholesterol levels, and suppressing inflammation would be to apply it in human trials. A potentially effective cocktail which could be developed would be a combination of hEP-HSA and other HCV drugs which target the virus itself. This cocktail could inhibit viral entry as well as viral replication if a protease inhibitor is present. The process

of analyzing the effects in humans would require many years of testing and studies in order to deem it safe and effective. One thing that must be determined is how the addition of hEP-HSA will affect the body's natural ability to degrade cholesterol and other lipids. Since apo E's natural function is in cholesterol transport, what kind of effect would hEP binding to the LDLR and HSPG have on the body? The body needs these receptors in order to clear cholesterol. Both the LDLR and HSPG present on the liver aid in the clearance of LDL cholesterol and triglycerides from plasma (61, 94). This must be determined before this fusion protein is approved for the market.

Overall, once we are able to successfully isolate and purify the recombinant proteins to highest degree possible, we will then be able to test the anti-viral effects without cytotoxicity.

BIBLIOGRAPHY

1. **Acton, S., A. Rigotti, K. T. Landschulz, S. Xu, H. H. Hobbs, and M. Krieger.** 1996. Identification of scavenger receptor SR-BI as a high density lipoprotein receptor. Science **271:**518-520.
2. **Agnello, V., G. Abel, M. Elfahal, G. B. Knight, and Q. X. Zhang.** 1999. Hepatitis C virus and other flaviviridae viruses enter cells via low density lipoprotein receptor. Proceedings of the National Academy of Sciences of the United States of America **96:**12766-12771.
3. **Aizaki, H., K. Morikawa, M. Fukasawa, H. Hara, Y. Inoue, H. Tani, K. Saito, M. Nishijima, K. Hanada, Y. Matsuura, M. M. Lai, T. Miyamura, T. Wakita, and T. Suzuki.** 2008. Critical role of virion-associated cholesterol and sphingolipid in hepatitis C virus infection. Journal of virology **82:**5715-5724.
4. **Akazawa, D., T. Date, K. Morikawa, A. Murayama, M. Miyamoto, M. Kaga, H. Barth, T. F. Baumert, J. Dubuisson, and T. Wakita.** 2007. CD81 expression is important for the permissiveness of Huh7 cell clones for heterogeneous hepatitis C virus infection. Journal of virology **81:**5036-5045.
5. **Allander, T., X. Forns, S. U. Emerson, R. H. Purcell, and J. Bukh.** 2000. Hepatitis C virus envelope protein E2 binds to CD81 of tamarins. Virology **277:**358-367.
6. **Andre, P., F. Komurian-Pradel, S. Deforges, M. Perret, J. L. Berland, M. Sodoyer, S. Pol, C. Brechot, G. Paranhos-Baccala, and V. Lotteau.** 2002. Characterization of low- and very-low-density hepatitis C virus RNA-containing particles. Journal of virology **76:**6919-6928.
7. **Andre, P., G. Perlemuter, A. Budkowska, C. Brechot, and V. Lotteau.** 2005. Hepatitis C virus particles and lipoprotein metabolism. Seminars in liver disease **25:**93-104.
8. **Appel, N., M. Zayas, S. Miller, J. Krijnse-Locker, T. Schaller, P. Friebe, S. Kallis, U. Engel, and R. Bartenschlager.** 2008. Essential role of do main III of nons tructural protein 5A for hepatitis C virus infectious particle assembly. PLoS pathogens **4:**e1000035.
9. **Barba, G., F. Harper, T. Harada, M. Kohara, S. Goulinet, Y. Matsuura, G. Eder, Z. Schaff, M. J. Chapman, T. Miyamura, and C. Brechot.** 1997. Hepatitis C virus core protein shows a cytoplasmic localization and associates to cellular lipid storage droplets. Proceedings of the National Academy of Sciences of the United States of America **94:**1200-1205.

10. **Barth, H., C. Schafer, M. I. Adah, F. Zhang, R. J. Linhardt, H. Toyoda, A. Kinoshita-Toyoda, T. Toida, T. H. Van Kuppevelt, E. Depla, F. Von Weizsacker, H. E. Blum, and T. F. Baumert.** 2003. Cellular binding of hepatitis C virus envelope glycoprotein E2 requires cell surface heparan sulfate. The Journal of biological chemistry **278:**41003-41012.
11. **Barth, H., E. K. Schnober, F. Zhang, R. J. Linhardt, E. Depla, B. Boson, F. L. Cosset, A. H. Patel, H. E. Blum, and T. F. Baumert.** 2006. Viral and cellular determinants of the hepatitis C virus envelope-heparan sulfate interaction. Journal of virology **80:**10579-10590.
12. **Bartosch, B., J. Dubuisson, and F. L. Cosset.** 2003. Infectious hepatitis C virus pseudo-particles containing functional E1-E2 envelope protein complexes. The Journal of experimental medicine **197:**633-642.
13. **Bartosch, B., A. Vitelli, C. Granier, C. Goujon, J. Dubuisson, S. Pascale, E. Scarselli, R. Cortese, A. Nicosia, and F. L. Cosset.** 2003. Cell entry of hepatitis C virus requires a set of co-receptors that include the CD81 tetraspanin and the SR-B1 scavenger receptor. The Journal of biological chemistry **278:**41624-41630.
14. **Basu, A., T. Kanda, A. Beyene, K. Saito, K. Meyer, and R. Ray.** 2007. Sulfated homologues of heparin inhibit hepatitis C virus entry into mammalian cells. Journal of virology **81:**3933-3941.
15. **Benedicto, I., F. Molina-Jimenez, B. Bartosch, F. L. Cosset, D. Lavillette, J. Prieto, R. Moreno-Otero, A. Valenzuela-Fernandez, R. Aldabe, M. Lopez-Cabrera, and P. L. Majano.** 2009. The tight junction-associated protein occludin is required for a postbinding step in hepatitis C virus entry and infection. Journal of virology **83:**8012-8020.
16. **Benga, W. J., S. E. Krieger, M. Dimitrova, M. B. Zeisel, M. Parnot, J. Lupberger, E. Hildt, G. Luo, J. McLauchlan, T. F. Baumert, and C. Schuster.** 2010. Apolipoprotein E interacts with hepatitis C virus nonstructural protein 5A and determines assembly of infectious particles. Hepatology **51:**43-53.
17. **Bertaux, C., and T. Dragic.** 2006. Different domains of CD81 mediate distinct stages of hepatitis C virus pseudoparticle entry. Journal of virology **80:**4940-4948.
18. **Blanchard, E., S. Belouzard, L. Goueslain, T. Wakita, J. Dubuisson, C. Wychowski, and Y. Rouille.** 2006. Hepatitis C virus entry depends on clathrin-mediated endocytosis. Journal of virology **80:**6964-6972.
19. **Boulant, S., C. Vanbelle, C. Ebel, F. Penin, and J. P. Lavergne.** 2005. Hepatitis C virus core protein is a dimeric alpha-helical protein exhibiting membrane protein features. Journal of virology **79:**11353-11365.
20. **Bu, G.** 2009. Apolipoprotein E and its receptors in Alzheimer's disease: pathways, pathogenesis and therapy. Nature reviews. Neuroscience **10:**333-344.
21. **Chang, K. S., J. Jiang, Z. Cai, and G. Luo.** 2007. Human apolipoprotein e is required for infectivity and production of hepatitis C virus in cell culture. Journal of virology **81:**13783-13793.
22. **Cheng, J. C., M. F. Chang, and S. C. Chang.** 1999. Specific interaction between the hepatitis C virus NS5B RNA polymerase and the 3' end of the viral RNA. Journal of virology **73:**7044-7049.

23. **Cheng, M., Y. Si, Y. Yang, X. Liu, Q. Gong, J. Zhao, Y. Niu, X. Li, Q. Jin, and W. Yang.** 2012. Recombinant human interleukin 28B: anti-HCV potency, receptor usage and restricted cell-type responsiveness. The Journal of antimicrobial chemotherapy **67:**1080-1087.
24. **Clarke, B.** 1997. Molecular virology of hepatitis C virus. The Journal of general virology **78 (Pt 10):**2397-2410.
25. **Codran, A., C. Royer, D. Jaeck, M. Bastien-Valle, T. F. Baumert, M. P. Kieny, C. A. Pereira, and J. P. Martin.** 2006. Entry of hepatitis C virus pseudotypes into primary human hepatocytes by clathrin-dependent endocytosis. The Journal of general virology **87:**2583-2593.
26. **Cohn, E. J., J. L. Oncley, L. E. Strong, W. L. Hughes, and S. H. Armstrong.** 1944. Chemical, Clinical, and Immunological Studies on the Products of Human Plasma Fractionation. I. The Characterization of the Protein Fractions of Human Plasma. The Journal of clinical investigation **23:**417-432.
27. **Connelly, M. A., and D. L. Williams.** 2003. SR-BI and cholesterol uptake into steroidogenic cells. Trends in endocrinology and metabolism: TEM **14:**467-472.
28. **Cormier, E. G., F. Tsamis, F. Kajumo, R. J. Durso, J. P. Gardner, and T. Dragic.** 2004. CD81 is an entry coreceptor for hepatitis C virus. Proceedings of the National Academy of Sciences of the United States of America **101:**7270-7274.
29. **Cregg, J. M., T. S. Vedvick, and W. C. Raschke.** 1993. Recent advances in the expression of foreign genes in Pichia pastoris. Biotechnology (N Y) **11:**905-910.
30. **Cun, W., J. Jiang, and G. Luo.** 2010. The C-terminal alpha-helix domain of apolipoprotein E is required for interaction with nonstructural protein 5A and assembly of hepatitis C virus. Journal of virology **84:**11532-11541.
31. **Drury, J., and V. Narayanaswami.** 2005. Examination of lipid-bound conformation of apolipoprotein E4 by pyrene excimer fluorescence. The Journal of biological chemistry **280:**14605-14610.
32. **Evans, M. J., T. von Hahn, D. M. Tscherne, A. J. Syder, M. Panis, B. Wolk, T. Hatziioannou, J. A. McKeating, P. D. Bieniasz, and C. M. Rice.** 2007. Claudin-1 is a hepatitis C virus co-receptor required for a late step in entry. Nature **446:**801-805.
33. **Feld, J. J., and J. H. Hoofnagle.** 2005. Mechanism of action of interferon and ribavirin in treatment of hepatitis C. Nature **436:**967-972.
34. **Flint, M., C. Maidens, L. D. Loomis-Price, C. Shotton, J. Dubuisson, P. Monk, A. Higginbottom, S. Levy, and J. A. McKeating.** 1999. Characterization of hepatitis C virus E2 glycoprotein interaction with a putative cellular receptor, CD81. Journal of virology **73:**6235-6244.
35. **Furuse, M., K. Fujita, T. Hiiragi, K. Fujimoto, and S. Tsukita.** 1998. Claudin-1 and -2: novel integral membrane proteins localizing at tight junctions with no sequence similarity to occludin. The Journal of cell biology **141:**1539-1550.
36. **Furuse, M., and S. Tsukita.** 2006. Claudins in occluding junctions of humans and flies. Trends in cell biology **16:**181-188.
37. **Gastaminza, P., S. B. Kapadia, and F. V. Chisari.** 2006. Differential biophysical properties of infectious intracellular and secreted hepatitis C virus particles. Journal of virology **80:**11074-11081.

38. **Germi, R., J. M. Crance, D. Garin, J. Guimet, H. Lortat-Jacob, R. W. Ruigrok, J. P. Zarski, and E. Drouet.** 2002. Cellular glycosaminoglycans and low density lipoprotein receptor are involved in hepatitis C virus adsorption. Journal of medical virology **68:**206-215.
39. **Gibbons, D. L., M. C. Vaney, A. Roussel, A. Vigouroux, B. Reilly, J. Lepault, M. Kielian, and F. A. Rey.** 2004. Conformational change and protein-protein interactions of the fusion protein of Semliki Forest virus. Nature **427:**320-325.
40. **Goffard, A., N. Callens, B. Bartosch, C. Wychowski, F. L. Cosset, C. Montpellier, and J. Dubuisson.** 2005. Role of N-linked glycans in the functions of hepatitis C virus envelope glycoproteins. Journal of virology **79:**8400-8409.
41. **Gosert, R., D. Egger, V. Lohmann, R. Bartenschlager, H. E. Blum, K. Bienz, and D. Moradpour.** 2003. Identification of the hepatitis C virus RNA replication complex in Huh-7 cells harboring subgenomic replicons. Journal of virology **77:**5487-5492.
42. **Grakoui, A., D. W. McCourt, C. Wychowski, S. M. Feinstone, and C. M. Rice.** 1993. A second hepatitis C virus-encoded proteinase. Proceedings of the National Academy of Sciences of the United States of America **90:**10583-10587.
43. **Hatters, D. M., C. A. Peters-Libeu, and K. H. Weisgraber.** 2005. Engineering conformational destabilization into mouse apolipoprotein E. A model for a unique property of human apolipoprotein E4. The Journal of biological chemistry **280:**26477-26482.
44. **Helle, F., A. Goffard, V. Morel, G. Duverlie, J. McKeating, Z. Y. Keck, S. Foung, F. Penin, J. Dubuisson, and C. Voisset.** 2007. The neutralizing activity of anti-hepatitis C virus antibodies is modulated by specific glycans on the E2 envelope protein. Journal of virology **81:**8101-8111.
45. **Herz, J., and U. Beffert.** 2000. Apolipoprotein E receptors: linking brain development and Alzheimer's disease. Nature reviews. Neuroscience **1:**51-58.
46. **Hijikata, M., H. Mizushima, T. Akagi, S. Mori, N. Kakiuchi, N. Kato, T. Tanaka, K. Kimura, and K. Shimotohno.** 1993. Two distinct proteinase activities required for the processing of a putative nonstructural precursor protein of hepatitis C virus. Journal of virology **67:**4665-4675.
47. **Hoofnagle, J. H.** 1997. Hepatitis C: the clinical spectrum of disease. Hepatology **26:**15S-20S.
48. **Huang, H., F. Sun, D. M. Owen, W. Li, Y. Chen, M. Gale, Jr., and J. Ye.** 2007. Hepatitis C virus production by human hepatocytes dependent on assembly and secretion of very low-density lipoproteins. Proceedings of the National Academy of Sciences of the United States of America **104:**5848-5853.
49. **Ji, Y., N. Wang, R. Ramakrishnan, E. Sehayek, D. Huszar, J. L. Breslow, and A. R. Tall.** 1999. Hepatic scavenger receptor BI promotes rapid clearance of high density lipoprotein free cholesterol and its transport into bile. The Journal of biological chemistry **274:**33398-33402.
50. **Jiang, J., W. Cun, X. Wu, Q. Shi, H. Tang, and G. Luo.** 2012. Hepatitis C Virus Attachment Mediated by Apolipoprotein E Binding to Cell Surface Heparan Sulfate. Journal of virology.
51. **Jiang, J., W. Cun, X. Wu, Q. Shi, H. Tang, and G. Luo.** 2012. Hepatitis C virus attachment mediated by apolipoprotein e binding to cell surface heparan sulfate. Journal of virology **86:**7256-7267.

52. **Jones, C. T., C. L. Murray, D. K. Eastman, J. Tassello, and C. M. Rice.** 2007. Hepatitis C virus p7 and NS2 proteins are essential for production of infectious virus. Journal of virology **81:**8374-8383.
53. **Jones, D. M., A. H. Patel, P. Targett-Adams, and J. McLauchlan.** 2009. The hepatitis C virus NS4B protein can trans-complement viral RNA replication and modulates production of infectious virus. Journal of virology **83:**2163-2177.
54. **Koutsoudakis, G., A. Kaul, E. Steinmann, S. Kallis, V. Lohmann, T. Pietschmann, and R. Bartenschlager.** 2006. Characterization of the early steps of hepatitis C virus infection by using luciferase reporter viruses. Journal of virology **80:**5308-5320.
55. **Levrero, M.** 2006. Viral hepatitis and liver cancer: the case of hepatitis C. Oncogene **25:**3834-3847.
56. **Lindenbach, B. D., and C. M. Rice.** 2005. Unravelling hepatitis C virus replication from genome to function. Nature **436:**933-938.
57. **Liu, S., W. Kuo, W. Yang, W. Liu, G. A. Gibson, K. Dorko, S. C. Watkins, S. C. Strom, and T. Wang.** 2010. The second extracellular loop dictates Occludin-mediated HCV entry. Virology **407:**160-170.
58. **Liu, S., K. D. McCormick, W. Zhao, T. Zhao, D. Fan, and T. Wang.** 2012. Human apolipoprotein E peptides inhibit hepatitis C virus entry by blocking virus binding. Hepatology.
59. **Liu, S., W. Yang, L. Shen, J. R. Turner, C. B. Coyne, and T. Wang.** 2009. Tight junction proteins claudin-1 and occludin control hepatitis C virus entry and are downregulated during infection to prevent superinfection. Journal of virology **83:**2011-2014.
60. **Ma, Y., J. Yates, Y. Liang, S. M. Lemon, and M. Yi.** 2008. NS3 helicase domains involved in infectious intracellular hepatitis C virus particle assembly. Journal of virology **82:**7624-7639.
61. **MacArthur, J. M., J. R. Bishop, K. I. Stanford, L. Wang, A. Bensadoun, J. L. Witztum, and J. D. Esko.** 2007. Liver heparan sulfate proteoglycans mediate clearance of triglyceride-rich lipoproteins independently of LDL receptor family members. The Journal of clinical investigation **117:**153-164.
62. **Mahley, R. W.** 1988. Apolipoprotein E: cholesterol transport protein with expanding role in cell biology. Science **240:**622-630.
63. **McLauchlan, J., M. K. Lemberg, G. Hope, and B. Martoglio.** 2002. Intramembrane proteolysis promotes trafficking of hepatitis C virus core protein to lipid droplets. The EMBO journal **21:**3980-3988.
64. **Meertens, L., C. Bertaux, L. Cukierman, E. Cormier, D. Lavillette, F. L. Cosset, and T. Dragic.** 2008. The tight junction proteins claudin-1, -6, and -9 are entry cofactors for hepatitis C virus. Journal of virology **82:**3555-3560.
65. **Meertens, L., C. Bertaux, and T. Dragic.** 2006. Hepatitis C virus entry requires a critical postinternalization step and delivery to early endosomes via clathrin-coated vesicles. Journal of virology **80:**11571-11578.
66. **Merz, A., G. Long, M. S. Hiet, B. Brugger, P. Chlanda, P. Andre, F. Wieland, J. Krijnse-Locker, and R. Bartenschlager.** 2011. Biochemical and morphological properties of hepatitis C virus particles and determination of their lipidome. The Journal of biological chemistry **286:**3018-3032.

67. **Mihaila, R., L. Nedelcu, O. Fratila, E. C. Rezi, C. Domnariu, R. Ciuca, A. V. Zaharie, A. Olteanu, L. Bera, and M. Deac.** 2009. Lovastatin and fluvastatin reduce viremia and the pro-inflammatory cytokines in the patients with chronic hepatitis C. Hepato-gastroenterology **56:**1704-1709.
68. **Modis, Y., S. Ogata, D. Clements, and S. C. Harrison.** 2004. Structure of the dengue virus envelope protein after membrane fusion. Nature **427:**313-319.
69. **Molina, S., V. Castet, C. Fournier-Wirth, L. Pichard-Garcia, R. Avner, D. Harats, J. Roitelman, R. Barbaras, P. Graber, P. Ghersa, M. Smolarsky, A. Funaro, F. Malavasi, D. Larrey, J. Coste, J. M. Fabre, A. Sa-Cunha, and P. Maurel.** 2007. The low-density lipoprotein receptor plays a role in the infection of pri mary human hepatocytes by hepatitis C virus. Journal of hepatology **46:**411-419.
70. **Monazahian, M., I. Bohme, S. Bonk, A. Koch, C. Scholz, S. Grethe, and R. Thomssen.** 1999. Low density lipoprotein receptor as a candidate receptor for hepatitis C virus. Journal of medical virology **57:**223-229.
71. **Moradpour, D., V. Brass, E. Bieck, P. Friebe, R. Gosert, H. E. Blum, R. Bartenschlager, F. Penin, and V. Lohmann.** 2004. Membrane association of the RNA-dependent RNA polymerase is essential for hepatitis C virus RNA replication. Journal of virology **78:**13278-13284.
72. **Moradpour, D., C. Englert, T. Wakita, and J. R. Wands.** 1996. Characterization of cell lines allowing tightly regulated expression of hepatitis C virus core protein. Virology **222:**51-63.
73. **Morikawa, K., Z. Zhao, T. Date, M. Miyamoto, A. Murayama, D. Akazawa, J. Tanabe, S. Sone, and T. Wakita.** 2007. The roles of CD81 and glycosaminoglycans in the adsorption and uptake of infectious HCV particles. Journal of medical virology **79:**714-723.
74. **Morita, K., M. Furuse, K. Fujimoto, and S. Tsukita.** 1999. Claudin multigene family encoding four-transmembrane domain protein components of tight junction strands. Proceedings of the National Academy of Sciences of the United States of America **96:**511-516.
75. **Nakano, T., G. M. Lau, M. Sugiyama, and M. Mizokami.** 2012. An updated analysis of hepatitis C virus genotypes and subtypes based on the complete coding region. Liver international : official journal of the International Association for the Study of the Liver **32:**339-345.
76. **Narayanaswami, V., J. N. Maiorano, P. Dhanasekaran, R. O. Ryan, M. C. Phillips, S. Lund-Katz, and W. S. Davidson.** 2004. Helix orientation of the functional domains in apolipoprotein e in discoidal high density lipoprotein particles. The Journal of biological chemistry **279:**14273-14279.
77. **Op De Beeck, A., C. Voisset, B. Bartosch, Y. Ciczora, L. Cocquerel, Z. Keck, S. Foung, F. L. Cosset, and J. Dubuisson.** 2004. Characterization of functional hepatitis C virus envelope glycoproteins. Journal of virology **78:**2994-3002.
78. **Osborn, B. L., H. S. Olsen, B. Nardelli, J. H. Murray, J. X. Zhou, A. Garcia, G. Moody, L. S. Zaritskaya, and C. Sung.** 2002. Pharmacokinetic and pharmacodynamic studies of a human serum albumin-interferon-alpha fusion protein in cynomolgus monkeys. The Journal of pharmacology and experimental therapeutics **303:**540-548.

79. **Paul, D., I. Romero-Brey, J. Gouttenoire, S. Stoitsova, J. Krijnse-Locker, D. Moradpour, and R. Bartenschlager.** 2011. NS4B self-interaction through conserved C-terminal elements is required for the establishment of functional hepatitis C virus replication complexes. Journal of virology **85:**6963-6976.
80. **Petracca, R., F. Falugi, G. Galli, N. Norais, D. Rosa, S. Campagnoli, V. Burgio, E. Di Stasio, B. Giardina, M. Houghton, S. Abrignani, and G. Grandi.** 2000. Structure-function analysis of hepatitis C virus envelope-CD81 binding. Journal of v irology **74:**4824-4830.
81. **Pileri, P., Y. Uematsu, S. Campagnoli, G. Galli, F. Falugi, R. Petracca, A. J. Weiner, M. Houghton, D. Rosa, G. Grandi, and S. Abrignani.** 1998. Binding of he patitis C virus to CD81. Science **282:**938-941.
82. **Pitha, J., T. Irie, P. B. Sklar, and J. S. Nye.** 1988. Drug solubilizers to aid pharmacologists: amorphous cyclodextrin derivatives. Life sciences **43:**493-502.
83. **Ploss, A., M. J. Evans, V. A. Gaysinskaya, M. Panis, H. You, Y. P. de Jong, and C. M. Rice.** 2009. Human occludin is a hepatitis C virus entry factor required for infection of mouse cells. Nature **457:**882-886.
84. **Popescu, C. I., N. Callens, D. Trinel, P. Roingeard, D. Moradpour, V. Descamps, G. Duverlie, F. Penin, L. Heliot, Y. Rouille, and J. Dubuisson.** 2011. NS2 protein of hepatitis C virus interacts with structural and non-structural proteins towards virus assembly. PLoS pathogens **7:**e1001278.
85. **Poynard, T., M. F. Yuen, V. Ratziu, and C. L. Lai.** 2003. Viral hepatitis C. Lancet **362:**2095-2100.
86. **Praefcke, G. J., and H. T. McMahon.** 2004. The dynamin superfamily: universal membrane tubulation and fission molecules? Nature reviews. Molecular cell biology **5:**133-147.
87. **Prince, A. M., T. Huima-Byron, T. S. Parker, and D. M. Levine.** 1996. Visualization of hepatitis C v irions and putative defective interfering particles isolated from low-density lipoproteins. Journal of viral hepatitis **3:**11-17.
88. **Sainz, B., Jr., N. Barretto, D. N. Martin, N. Hiraga, M. Imamura, S. Hussain, K. A. Marsh, X. Yu, K. Chayama, W. A. Alrefai, and S. L. Uprichard.** 2012. Identification of the Niemann-Pick C1-like 1 cholesterol absorption receptor as a new hepatitis C virus entry factor. Nature medicine **18:**281-285.
89. **Sakai, A., M. S. Claire, K. Faulk, S. Govindarajan, S. U. Emerson, R. H. Purcell, and J. Bukh.** 2003. The p7 polypeptide of hepatitis C virus is critical for infectivity and contains functionally important genotype-specific sequences. Proceedings of the National Academy of Sciences of the United States of America **100:**11646-11651.
90. **Santolini, E., G. Migliaccio, and N. La Monica.** 1994. Biosynthesis and biochemical properties of the hepatitis C virus core protein. Journal of virology **68:**3631-3641.
91. **Steinmann, E., F. Penin, S. Kallis, A. H. Patel, R. Bartenschlager, and T. Pietschmann.** 2007. Hepatitis C virus p7 protein is crucial for assembly and release of infectious virions. PLoS pathogens **3:**e103.
92. **Susser, S., C. Welsch, Y. Wang, M. Zettler, F. S. Domingues, U. Karey, E. Hughes, R. Ralston, X. Tong, E. Herrmann, S. Zeuzem, and C. Sarrazin.** 2009. Characterization of resistance to the protease inhibitor boceprevir in hepatitis C virus-infected patients. Hepatology **50:**1709-1718.

93. **Tellinghuisen, T. L., K. L. Foss, and J. Treadaway.** 2008. Regulation of hepatitis C virion production via phosphorylation of the NS5A protein. PLoS pathogens **4:**e1000032.
94. **Tolleshaug, H., J. L. Goldstein, W. J. Schneider, and M. S. Brown.** 1982. Posttranslational processing of the LDL receptor and its genetic disruption in familial hypercholesterolemia. Cell **30:**715-724.
95. **Tscherne, D. M., C. T. Jones, M. J. Evans, B. D. Lindenbach, J. A. McKeating, and C. M. Rice.** 2006. Time- and temperature-dependent activation of hepatitis C virus for low-pH-triggered entry. Journal of virology **80:**1734-1741.
96. **Tsukiyama-Kohara, K., N. Iizuka, M. Kohara, and A. Nomoto.** 1992. Internal ribosome entry site within hepatitis C virus RNA. Journal of virology **66:**1476-1483.
97. **Vieyres, G., X. Thomas, V. Descamps, G. Duverlie, A. H. Patel, and J. Dubuisson.** 2010. Characterization of the envelope glycoproteins associated with infectious hepatitis C virus. Journal of virology **84:**10159-10168.
98. **Voisset, C., N. Callens, E. Blanchard, A. Op De Beeck, J. Dubuisson, and N. Vu-Dac.** 2005. High density lipoproteins facilitate hepatitis C virus entry through the scavenger receptor class B type I. The Journal of biological chemistry **280:**7793-7799.
99. **Wakita, T., T. Pietschmann, T. Kato, T. Date, M. Miyamoto, Z. Zhao, K. Murthy, A. Habermann, H. G. Krausslich, M. Mizokami, R. Bartenschlager, and T. J. Liang.** 2005. Production of infectious hepatitis C virus in tissue culture from a cloned viral genome. Nature medicine **11:**791-796.
100. **Wang, C., P. Sarnow, and A. Siddiqui.** 1993. Translation of human hepatitis C virus RNA in cultured cells is mediated by an internal ribosome-binding mechanism. Journal of virology **67:**3338-3344.